Journal of Structural Geology 43 (2012) 73–91

Contents lists available at SciVerse ScienceDirect

Journal of Structural Geology

journal homepage: www.elsevier.com/locate/jsg

An alternative emplacement model for the classic Ardnamurchan cone sheet swarm, NW Scotland, involving lateral magma supply via regional dykes

Craig Magee [a,b,*], Carl Stevenson [a], Brian O'Driscoll [c], Nick Schofield [a], Ken McDermott [a]

[a] School of Geography, Earth and Environmental Science, University of Birmingham, Edgbaston, Birmingham B15 2TT, UK
[b] Department of Earth Science and Engineering, Imperial College, London SW7 2BP, UK
[c] School of Physical and Geographical Sciences, Keele University, Keele ST5 5BG, UK

ARTICLE INFO

Article history:
Received 17 November 2011
Received in revised form
1 August 2012
Accepted 3 August 2012
Available online 17 August 2012

Keywords:
Anisotropy of magnetic susceptibility
Ardnamurchan
Cone sheets
Inclined sheets
Regional dykes

ABSTRACT

Sub-volcanic intrusive networks, of which cone sheets are recognised as a major constituent, partially control volcano growth and eruption style. The accepted cone sheet model is that these confocally dipping intrusions originate from an unexposed central magma chamber through dip-parallel magma flow. However, the emplacement mechanism of cone sheets remains poorly understood. The ~58 Ma cone sheet swarm of Ardnamurchan, NW Scotland, offers an excellent opportunity to further resolve the emplacement dynamics of cone sheets, through studying magma flow, and their importance in volcanic edifice construction. Structural measurements and anisotropy of magnetic susceptibility (AMS) analyses have constrained a lateral magma flow pattern, consistently oriented NW–SE, in the majority of the Ardnamurchan cone sheets. Field observations also highlight the importance of host rock structure and interference between competing local and regional stress fields in controlling intrusion geometry. Our observations suggest cone sheet formation may be linked to laterally propagating NW–SE trending regional dykes, sourced from laterally adjacent magmatic systems (likely the Palaeogene Mull Central Complex), which are deflected around the central complex by stress field interference. Implicitly, edifice construction and potential eruption precursors observed at a volcano may instigate, or result from, magmatic activity in laterally adjacent volcanic systems.

1. Introduction

Discerning the emplacement mechanisms of sheet intrusions is key to understanding the transport, delivery and accommodation of magma in the upper crust. Inwardly inclined conical intrusions (cone sheets) are closely associated with ring dykes and are recognised as important elements in the intrusive framework of many volcanic systems in the geological record (e.g. Mull Central Complex, Scotland, Bailey et al., 1924; Tejeda complex, Gran Canaria, Schirnick et al., 1999; Thverartindur igneous centre, Iceland, Klausen, 2004; Otoge igneous complex, Japan, Geshi, 2005). Reconstructing the growth and temporal evolution of conical intrusions (both cone sheets and ring dykes) is therefore an important step in understanding the sub-edifice behaviour of volcanic systems (e.g. Eastern Mourne Centre, N Ireland, Stevenson et al., 2007a; Stardalur Volcano, Iceland, Pasquarè and Tibaldi, 2007; Tibaldi and Pasquarè, 2008).

The propagation and geometry of sheet intrusions within the upper crust is controlled by the contemporaneous regional and local stress regimes, the magma dynamics and the behaviour and pre-existing structure of the host rock (Pollard, 1987; Rubin, 1995; Geshi, 2005; Gudmundsson and Phillip, 2006; Acocella and Neri, 2009; Siler and Karson, 2009; Schofield et al., 2010). Cone sheet development is traditionally interpreted to occur in three stages: (1) build-up of magma overpressure within a central source chamber imparts a local stress field on the host rock that (2) favours the formation of new inverted conical fractures (Fig. 1b). (3) Intrusion of magma radially upwards and outwards (Palmer et al., 2007) along these tensile fractures forms cone sheets and releases the overpressure (Fig. 1b; Bailey et al., 1924; Anderson, 1936). Here, we test the emplacement of the Palaeogene cone sheets of Ardnamurchan, NW Scotland (Fig. 1a), using anisotropy of magnetic susceptibility (AMS) to determine magma flow pathways. Our data indicate that sub-horizontal to moderately plunging magnetic lineations, interpreted as parallel to the primary magma flow axes, dominate the magnetic fabrics of the Ardnamurchan cone sheets. This suggests that Ardnamurchan cone sheet emplacement was either more complicated than previous models

* Corresponding author. Department of Earth Science and Engineering, Imperial College, London SW7 2BP, UK.
E-mail address: c.magee@imperial.ac.uk (C. Magee).

0191-8141
http://dx.doi.org/10.1016/j.jsg.2012.08.004

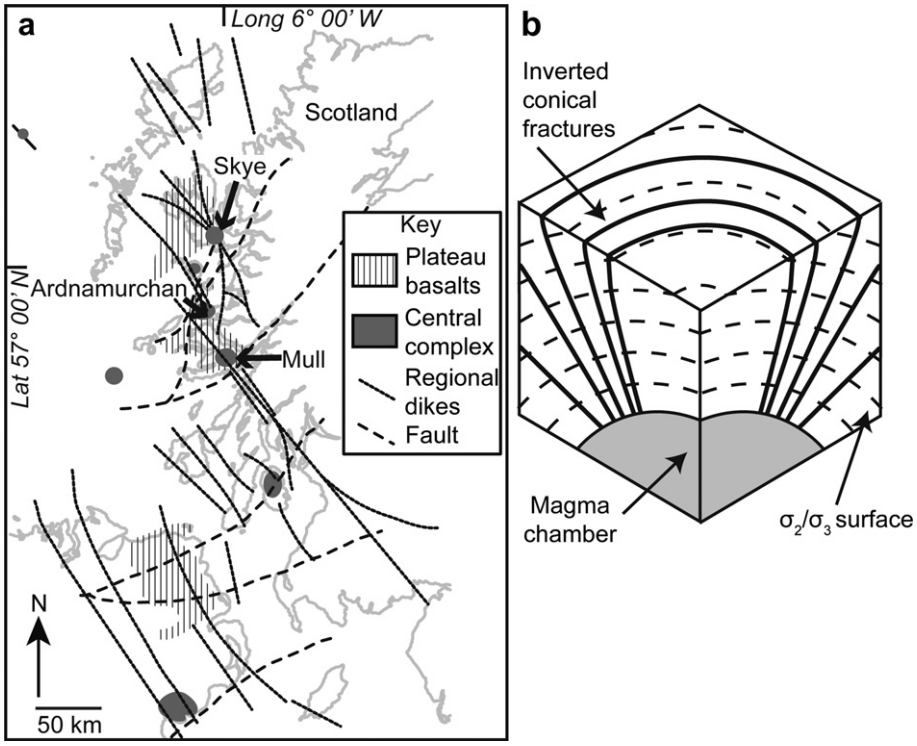

Fig. 1. (a) Map of the British and Irish Palaeogene Igneous Province highlighting the positions of plateau basalts, central complexes (including Ardnamurchan, Mull and Skye) and the NW–SE regional dyke swarm (after Emeleus and Bell, 2005). (b) Cone sheet emplacement model (after Anderson, 1936) where overpressure within the magma chamber imparts a local stress field favouring formation of new inverted conical fractures, intruded to form cone sheets.

imply (i.e. in order to maintain a central source) or that they may be laterally fed from an adjacent magma source. We also emphasise the influence of the pre-existing host rock structure and the interaction between local and regional stress fields in controlling cone sheet geometry. Overall, we provide a physical model that suggests geographical proximity is not necessarily indicative of magmatic cogenesis.

2. Previous work

The original emplacement model for cone sheets is based principally on the geometries of cone sheets from the Palaeogene Mull (Bailey et al., 1924) and Ardnamurchan (Fig. 2; Richey and Thomas, 1930) Central Complexes, NW Scotland. Subsequent variations on this cone sheet emplacement model have primarily focused on the effects of magma intrusion into shear fractures as opposed to tensile fractures (e.g. Durrance, 1967; Phillips, 1974), changes to the controlling stress regime temporally (e.g. Walker, 1993; Schirnick et al., 1999; Tibaldi and Pasquarè, 2008), different source magma chamber shapes (Gudmundsson, 1998; Schirnick et al., 1999; Klausen, 2004) and variable host rock characteristics (Gudmundsson, 2002; Tibaldi and Pasquarè, 2008). However, all models adopt the same fundamental assumptions of Anderson's (1936) model and predict: 1) Cone sheets have a roughly concentric or elliptical strike; 2) dip inwards to a common central source at depth (Siler and Karson, 2009); 3) and from this source, magma flow radiates upwards and outwards (Palmer et al., 2007). Hereafter we avoid the genetic term 'cone sheet' and adopt instead the descriptive term 'inclined sheets' to avoid any inherent implications for emplacement mechanism (cf. Gautneb et al., 1989; Gautneb and Gudmundsson, 1992; Siler and Karson, 2009).

Over the last 30 years, ring dyke emplacement has been re-evaluated. Using detailed field structural observations and published geophysical data, Day (1989) re-interpreted the Hypersthene Gabbro ring dyke on Ardnamurchan as a laccolith. Similarly, AMS studies of magmatic flow patterns coupled with field observations have lead to the re-interpretation of other classic ring dykes as either lopoliths or laccoliths (e.g. the Great Eucrite, Ardnamurchan, NW Scotland, O'Driscoll et al., 2006; the Eastern Mourne Centre, N Ireland, Stevenson et al., 2007a). Only a few studies have, however, adopted similar quantitative approaches to delineating the source of inclined sheet swarms. Herrero-Bervera et al. (2001) conducted an AMS study of the dykes and inclined sheets of the Cuillin complex, Skye, and determined a consistent magma flow pattern suggestive of a common central source. A similar result has been presented for the inclined sheets and parallel dyke swarm of the Otoge igneous complex, Japan, interpreted from geochemical data and magma flow indicators such as vesicle imbrications and slickenlines (Geshi, 2005).

3. The Ardnamurchan inclined sheets

The British and Irish Paleogene Igneous Province (BIPIP) formed through extensive igneous activity between ca. 61 and 55 Ma, during the opening of the North Atlantic (Emeleus and Bell, 2005). Much of the voluminous flood basalt lavas have eroded away exposing a shallow (<5 km depth) intrusive network of sills, central complexes (e.g. Ardnamurchan) and NW–SE striking regional dykes (Fig. 1a; Emeleus and Bell, 2005). The geometry of the regional dykes, which were intruded contemporaneously to central complex construction (Emeleus and Bell, 2005), indicates regional extension oriented NE–SW occurred throughout the formation of the BIPIP (England, 1988). The central complexes, which represent the deeply eroded roots of ancient volcanic edifices, often display evidence of multiple phases of igneous activity and hence a complex history of fluctuating extensional and

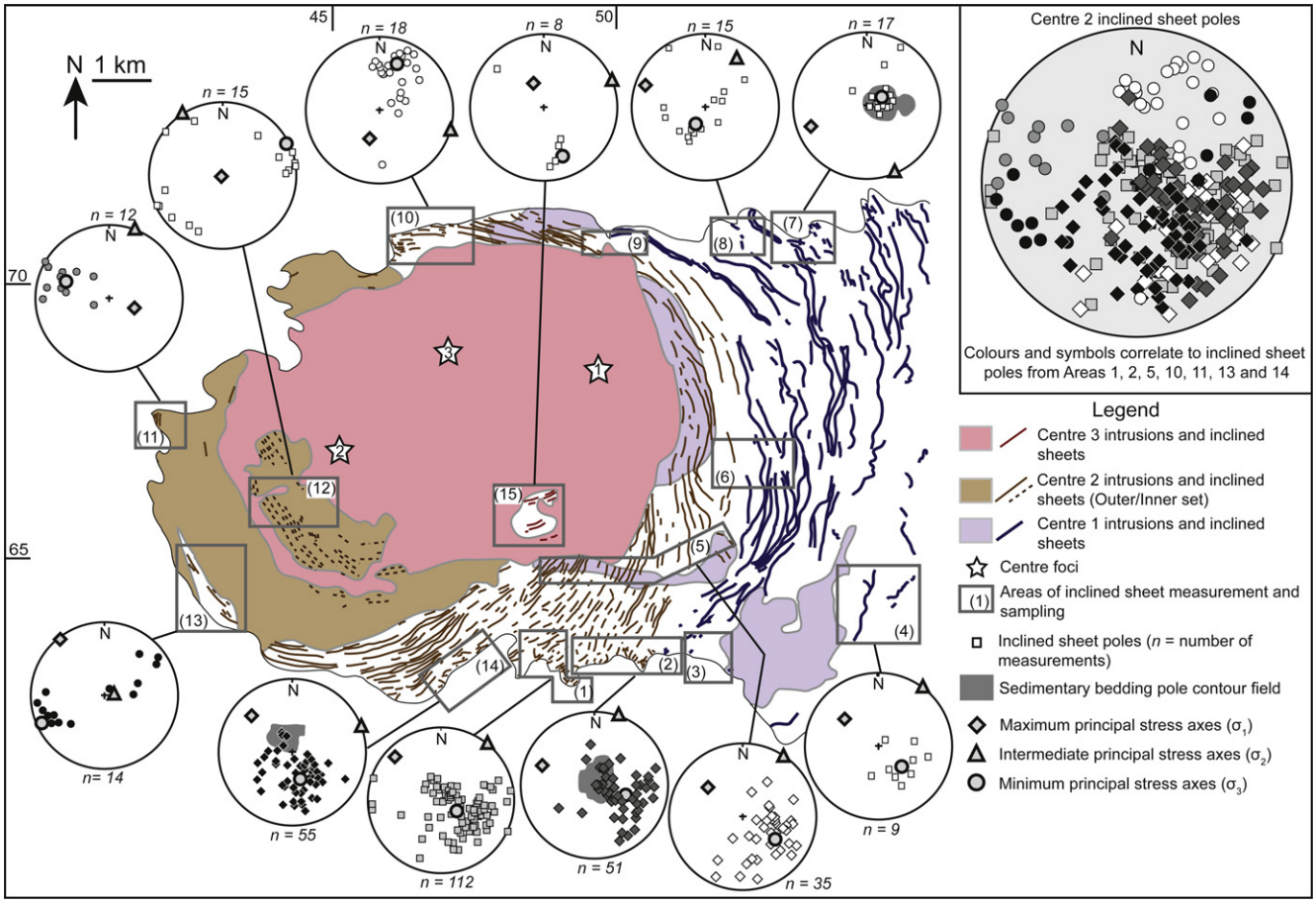

Fig. 2. Detailed map of Ardnamurchan depicting accentuated inclined sheet strikes. Areas of main data collection are shown (adapted from Richey and Thomas, 1930; Emeleus, 2009). Equal-area lower-hemisphere stereoplots of inclined sheet poles are presented highlighting their variability in dip value and dip azimuth, although on average their dip disposition is towards the central complex. A combined plot of all Outer Centre 2 inclined sheet poles is inset. Bedding pole contour fields and principal stress axes, resolved from the inclined sheet poles, are also displayed. The σ_1 stress axes are often oriented towards the central complex and become steeper as proximity to the centre increases, indicating a radially inwardly inclined orientation. Conversely, σ_3 becomes shallower with distance from the central complex. Grid references refer to the UK National Grid co-ordinate system.

compressional stress regimes associated with the regional tectonics and magma chamber inflation and deflation (Bailey et al., 1924; Richey and Thomas, 1930; England, 1988; Day, 1989; Emeleus and Bell, 2005).

Richey and Thomas (1930) first described the classic 'cone-sheets' of Ardnamurchan, mapping their concentric strike and inward dips (10–70°), which steepen towards the centre (Fig. 2). The dolerite inclined sheets and a set of NW–SE trending dykes are intruded into domed country rocks (sedimentary bedding dips outwards from the central complex), including thinly-bedded Neoproterozoic Moine psammites and semi-pelites, interbedded Mesozoic limestones and siltstones, poorly consolidated Early Palaeogene volcaniclastics and basalts and some gabbroic intrusions (Fig. 2; Richey and Thomas, 1930; Emeleus and Bell, 2005). The inclined sheets, which have been grouped into four distinct suites based on their dip foci and age relationships with associated major gabbroic intrusions of the central complex (Fig. 2), were used to define three spatially and temporally separate centres of migratory intrusive activity in Ardnamurchan (Centres 1–3 progressively; Richey and Thomas, 1930).

The Centre 1 inclined sheets (attributed to the oldest Centre based on their dip foci) are not observed to be cross-cut by purportedly younger inclined sheets or major intrusions (Fig. 2; Richey and Thomas, 1930; Day, 1989). Inclined sheet intrusions adjacent to the major intrusions, particularly the Centre 2 Hypersthene Gabbro, record a complex history of intermittent intrusion throughout the evolution of the Ardnamurchan Central Complex (Day, 1989). For example, some inclined sheets of the Outer Centre 2 suite are cut by the major Centre 2 intrusions (Fig. 2), whilst others display specific contact metamorphic mineral assemblages linked to discrete phases in the growth of the Centre 2 Hypersthene Gabbro (Day, 1989). Contact metamorphism of the Neoproterozoic and Mesozoic country rock is also evidenced, from the development of a weak cleavage (i.e. sub-parallel to bedding) and the annealing of pre-existing fractures and bedding planes (Day, 1989). Adjacent to the Centre 2 Hypersthene Gabbro, field relationships indicate inclined sheet intrusion was associated with thrust faulting, whilst extensional, inward-dipping concentric normal faults developed during periods of inclined sheet quiescence (Day, 1989). A small number of inclined sheets, particularly those belonging to the Inner Centre 2 suite, cross-cut major gabbroic intrusions (e.g. the Hypersthene Gabbro, the Sgurr nam Meann ring dyke and the Garbh-dhail ring intrusion; Emeleus, 2009) of the central complex (Fig. 2). The Centre 3 inclined sheets are typically restricted to a screen of Early Palaeogene volcaniclastics and basalts within the Great Eucrite lopolith, although a small number of them is observed to cross-cut the gabbro as well (Fig. 2; Emeleus, 2009).

4. Sheet geometry and structural relationships

Structural measurements and oriented samples for magnetic analysis, were collected from outcrops representing the complete variety of the Ardnamurchan inclined sheets so that all ages, geometries and dip dispositions of outcropping inclined sheets were analysed (Fig. 2; see Supplementary Table 1). Over 500 structural data were collected from 242 inclined sheets, with multiple readings from single inclined sheets often recorded along strike or up/down the dip azimuth if local variations were observed. Where outcrop is intermittent, individual inclined sheets were identified by tracing chilled margins and correlating subtle grain-size variations. Iron-sulphide populations that are texturally consistent within single sheets but differ compared to other inclined sheets were also used to differentiate separate intrusions, assuming that the Fe-sulphides were leached from the host rock during the intrusion of individual sheets. This is supported by the identification of a biological signature within pyrite through geochemical analyses (e.g. standard mass spectrometry and *in situ* laser combustion; Prof. John Parnell, pers. comm.). To allow for easier data correlation, most inclined sheets measured and sampled have been placed into 15 groups, defined by their geographical proximity and relative ages (Fig. 2). The inclined sheets of the Outer Centre 2 set form the majority of the studied sheets (198 in total), as they are the best and most widely exposed inclined sheets on Ardnamurchan (Richey and Thomas, 1930).

4.1. Behaviour of the host rock during inclined sheet intrusion

Emplacement of magma within the upper crust is typically facilitated by the development or reactivation (e.g. bedding plane anisotropies, faults) of brittle fractures ahead of a propagating magma tip (Pollard and Johnson, 1973; Delaney et al., 1986; Rickwood, 1990; Rubin, 1995; Kavanagh et al., 2006; Menand, 2008). Intrusive sheets emplaced in a brittle regime primarily intrude orthogonally to the least compressive principal stress axis (i.e. σ_3; Anderson, 1951; Baer, 1995) when the internal magma pressure exceeds the magnitude of σ_3 (Delaney et al., 1986; Rubin, 1995). The orientation of the principal stress axes during intrusion therefore controls the orientation of new fractures or which, if any, pre-existing fractures may be reactivated and consequently dictates the geometry of sheet intrusions (Delaney et al., 1986). However, an increasing amount of evidence also demonstrates that in upper crustal magmatic systems, intrusion may occasionally instigate non-brittle behaviour of the host rocks (e.g. Thomson, 2007; Schofield et al., 2010, 2012). The morphology of intrusions exploiting non-brittle weaknesses in the host rock is distinct compared to those facilitated by brittle processes alone (Schofield et al., 2012); as explained in the next section. Determining host rock behaviour during emplacement of the Ardnamurchan inclined sheets therefore provides an important context to the structural measurements.

4.1.1. Evidence of brittle behaviour

Several structures associated with many Ardnamurchan inclined sheets suggest emplacement occurred within a brittle regime. For example, xenoliths entrained in inclined sheets are often elongated (5–60 cm in length), sub-angular to angular (Fig. 3a) and locally derived (i.e. xenolith lithology is comparable to that adjacent to the host intrusion). Other features associated to brittle host rock behaviour commonly observed in the Ardnamurchan inclined sheets, particularly those intruding Mesozoic metasedimentary rocks, are intrusive steps and broken bridges (Fig. 3b; Day, 1989). Schofield et al. (2012) provide a detailed and illustrated explanation of the brittle processes involved in broken bridge and intrusive step formation.

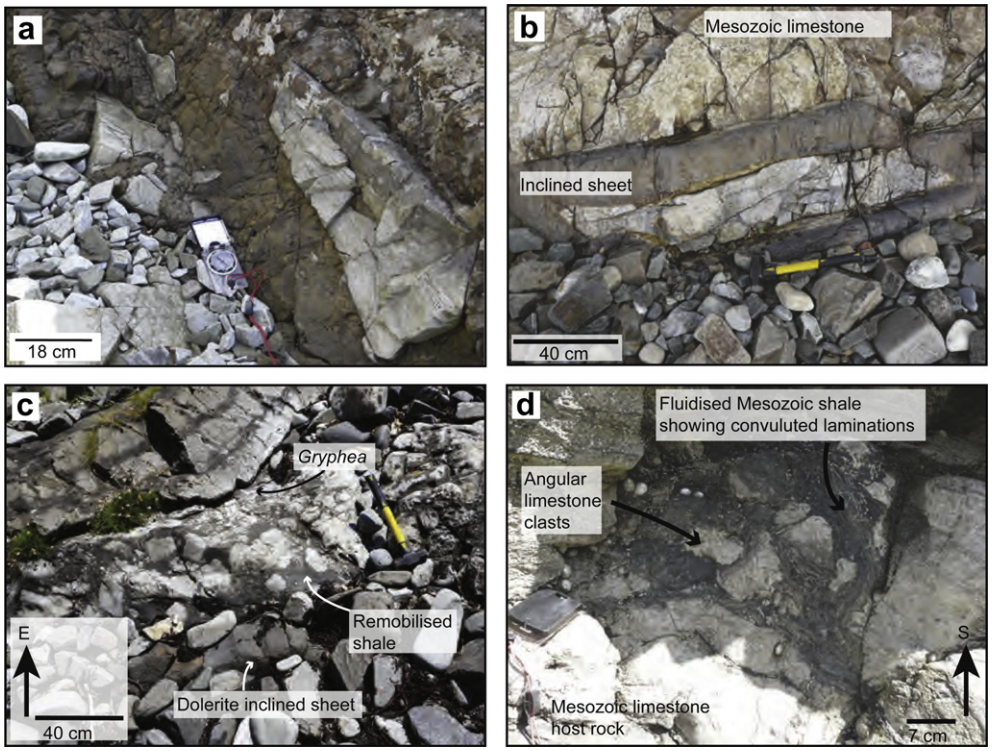

Fig. 3. (a) Angular xenoliths of Neoproterozoic Moine metasedimentary rock [NM 49177 62852]. (b) Mesozoic limestone broken bridge within an inclined sheet [NM 4957 62378]. (c) Remobilised Mesozoic shale adjacent to an inclined sheet and containing brecciated limestone and *Gryphea* fossils [NM 5301 5309]. (d) Fluidised Mesozoic shale containing brecciated limestone clasts and convoluted laminations [NM 53501 70778].

4.1.2. Non-brittle host rock behaviour

On Ardnamurchan, morphological features of several inclined sheets and associated host rock structures are suggestive of intrusion facilitated by non-brittle fluidisation processes. Host rock fluidisation may occur when rapidly expanding, heated fluids, derived either from the magma or the host rock pore fluid, infiltrate coherent host rock resulting in grain disaggregation and fluidisation (Kokelaar, 1992; Curtis and Riley, 2003; Schofield et al., 2010, 2012). Evidence of this process is observed surrounding several inclined sheets intruding Mesozoic metasedimentary rocks. Fig. 3c shows fragments of brecciated limestone and *Gryphaea* fossils enclosed within remobilised shale adjacent to an inclined sheet contact. Similarly, remobilised shale displaying conspicuous convoluted laminations and brecciated limestone clasts is also observed in host rock fractures adjacent to inclined sheets (Fig. 3d). In the latter case, intersection of a propagating fluid-filled tip cavity ahead of an intrusive sheet with a pre-existing fracture may have resulted in a sudden decrease in pressure, instigating fluidisation (Schofield et al., 2012). Schofield et al. (2012) describe an inclined sheet on the eastern flank of Ben Hiant that is divisible into a series of magma fingers and magma lobes, further evidence of non-brittle behaviour of the host rock during intrusion.

4.2. Structural measurements of the Ardnamurchan inclined sheets

Whilst there is evidence that the emplacement of some inclined sheets was facilitated by non-brittle processes, these are volumetrically minor and spatially restricted. Brittle processes can therefore be considered to dominate. The structural measurements of the Ardnamurchan inclined sheets are presented in Figs. 2, 4 and 5 (and in Supplementary Table 1).

4.2.1. Inclined sheet abundance

Although the concentric disposition of the Ardnamurchan inclined sheets is incomplete, with many inclined sheets supposedly located offshore or obscured by later major intrusions, there is an apparent increase in inclined sheet abundance to the south and south-east of the Ardnamurchan Central Complex (Fig. 2; Richey and Thomas, 1930). Out of the 198 Outer Centre 2 inclined sheets analysed in this study, 152 were observed to the south and south-east of the Ardnamurchan Central Complex (between Sròn Bheag and Mingary Castle). Whilst this distribution may not be definitive and possibly a result of poor exposure or measurement bias, similar geographically restricted areas of increased inclined sheet intensity have been observed at other central complexes (e.g. Skye, NW Scotland, Walker, 1993; Thverartindur, Iceland, Klausen, 2004; Otoge, Japan, Geshi, 2005).

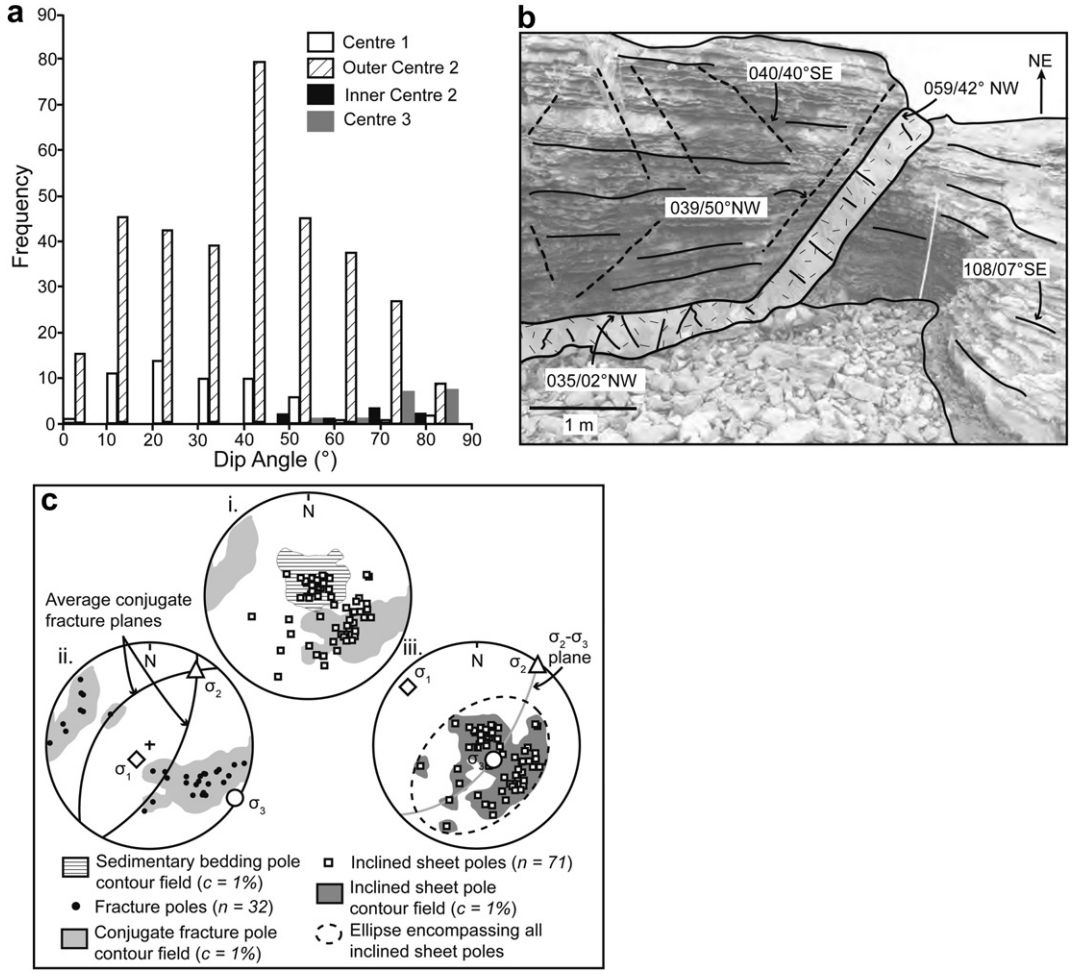

Fig. 4. (a) Dip versus frequency plot for the Ardnamurchan inclined sheets. (b) Transgressive sheet intruding bedding and also ramping up stratigraphy parallel to a series of inward-dipping fractures, one half of a conjugate fracture set (dashed lines) [NM 49240 62694]. (c) i) Equal-area stereographic projection of inclined sheet poles, conjugate fracture pole contours and bedding pole contours from Area 1 (Fig. 2). ii) Resolved formational principal stress axes orientations for conjugate fractures and iii) inclined sheet intrusion.

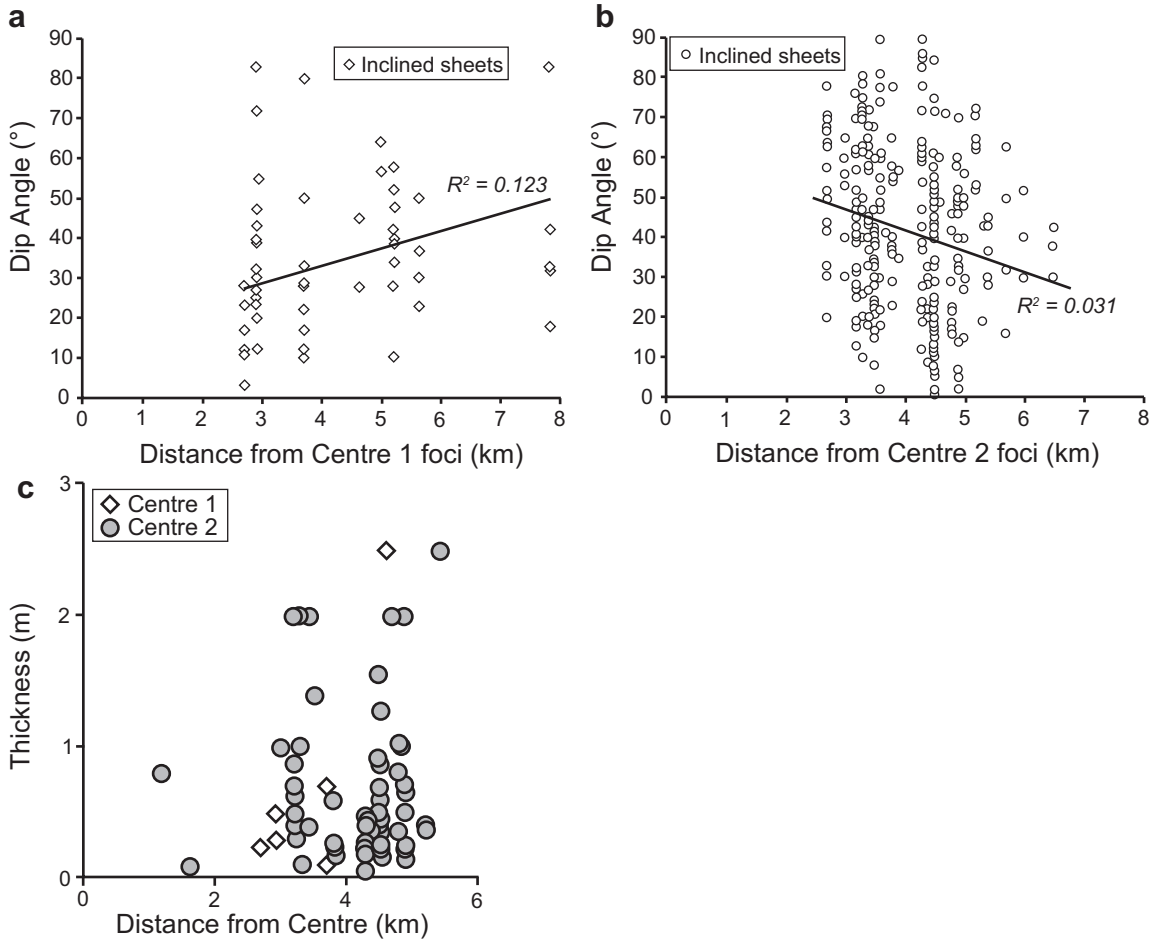

Fig. 5. (a) and (b) Plots of inclined sheet dip against distance from Centre 1 and 2 respectively. (c) A weak positive correlation between inclined sheet thickness and distance from the central complex.

4.2.2. Inclined sheet orientation

Individual inclined sheets are often discontinuous along strike on a decametre scale (Keunen, 1937), although a few inclined sheets observed inland at Sròn Bheag (Day, 1989) and on the east flank of Beinn nan Leathaid may be traced along strike for 0.1–1 km. Overall, a concentric strike is apparent from the mapped inclined sheet trend, which is generally supported by the inward convergence and concentric disposition of the poles to inclined sheet planes for the Outer Centre 2 and Centre 1 inclined sheet sets (Fig. 2; cf. Tibaldi et al., 2011). Approximately 2 km to the east and north-east of the Ardnamurchan Central Complex, the inclined sheet strike appear to be elongated NW–SE and wrap around the central complex (Fig. 2). Fig. 2 displays the equal-area, lower-hemisphere stereographic projections of inclined sheet poles measured for each area. Whilst the majority of inclined sheet dip azimuths is oriented radially towards the Ardnamurchan Central Complex, they often do not correlate to the Centre foci (particularly Centre 1) with which they were suggested by Richey and Thomas (1930) to define (Fig. 2). Out of all the inclined sheet dip azimuths measured (Centre 1 $n = 46$; Centre 2 $n = 320$; Centre 3 $n = 8$), only 50% from Centre 1 and Centre 2 (and 86% from Centre 3) may be projected to within 30° (to either side) of their respective foci positions.

4.2.3. Inclined sheet dip

Inclined sheets may have curved profiles in cross-section (cf. Anderson, 1936; Phillips, 1974), complicating dip correlations if significant variations in height above sea level are recorded for separate outcrops (Gautneb et al., 1989; Gautneb and Gudmundsson, 1992; Schirnick et al., 1999; Tibaldi et al., 2011). However, the Ardnamurchan inclined sheets are considered to approximately represent a single level within the ~5 km deep (Richey and Thomas, 1930) sub-volcanic system as the variation in altitude of inclined sheet outcrops is typically <350 m (i.e. from the coast to the peak of Beinn nan Leathaid).

From the inclined sheet pole distribution in the equal-area, lower-hemisphere stereographic projections displayed in Fig. 2, it is apparent that in some areas (e.g. Area 1, 2 and 10) two populations of inclined sheets may potentially be defined; one that dips inwards and another that dips outwards. Despite this and the wide range of dip angles (0–90°) measured for the Ardnamurchan inclined sheets, the mean dips (including both inward- and outward-dipping sheets) calculated for the Centre 1 (34°), Outer Centre 2 (42°), Inner Centre 2 (77°) and Centre 3 (59°) inclined sheet sets are similar to those presented by Richey and Thomas (1930) (i.e. 10–20°, 35–45°, 70°, 50° respectively). These calculated means are corroborated by plotting frequency against dip angle, which for Centre 1, Inner Centre 2 and Centre 3 inclined sheet sets reveals a Gaussian distribution (Fig. 4a). The bimodal distribution of the Outer Centre 2 inclined sheet set, with peaks at 10–20° and 40–50° (Fig. 4a), is similar to that observed in data from inclined sheet swarms in Iceland and is typically interpreted to reflect inclined sheet intrusion from different levels of a central magma reservoir (cf. Gautneb et al., 1989; Gudmundsson, 1995;

Burchardt and Gudmundsson, 2009). Whilst this may be the case for the Outer Centre 2 inclined sheet set, it is notable that the poles to the inclined sheets producing the peak at ~10° are located in a relatively tight cluster on the equal-area, lower-hemisphere projections and overlap with the range of locally measured bedding plane poles (Fig. 2). This implies that rather than a true bimodal distribution (*sensu* Gautneb et al., 1989), the ~10° peak likely represents inclined sheets which have intruded sub-parallel to outward-dipping bedding plane anisotropies (Day, 1989). Day (1989) noted that a significant proportion of the low angle inclined sheets deviate slightly (≤5°) from this bedding-parallel trend, similar to the angular difference between bedding and cleavage in the Neoproterozoic Moine and Mesozoic host rocks.

Field relationships reveal that the inward-dipping and outward-dipping inclined sheets do not represent two separate intrusion populations as numerous inclined sheets sub-parallel to bedding are observed to abruptly transgress up stratigraphy along inwardly inclined (25–65°) ramps (Fig. 4b) (Day, 1989). Fig. 4b and c illustrates a typical example from the south coast of Ardnamurchan (Area 1), where an inclined sheet is intruded sub-parallel to the Mesozoic limestone and shale bedding and also exhibits a ramp section oriented sub-parallel to a set of inwardly inclined fractures (~295/53° azimuth). The inward-dipping fractures, parallel to the inclined sheet ramps, form a conjugate pair with an outward-dipping set (~135/68° azimuth) that are not intruded (Fig. 4c). Where observed, portions of inclined sheets abutting an outward-dipping fracture, or the conjugate set, are distinctly chilled. Outward-dipping inclined sheets roughly concordant to bedding are predominantly observed ≥1 km from the outer margins of the Ardnamurchan Central Complex (Fig. 2), proportionally increasing with distance towards the furthest limits of significant Mesozoic metasedimentary rock outcrops (i.e. Area 7). Areas closer to the Ardnamurchan Central Complex also contain outward-dipping inclined sheets, although their abundance is significantly diminished and their inclination is often steeper (~56°). For example, re-investigation of the Inner Centre 2 inclined sheet set, which intrudes the major gabbroic intrusions of Centre 2 (Fig. 2), reveals that although a few sheets (~13%) dip inwards between 50° and 70° (cf. Richey and Thomas, 1930), the majority of sheets is sub-vertical (71–90°) with both inward and outward inclinations. This suggests they are dykes *sensu lato*.

Plots of inclined sheet dip angle against outcrop distance from the respective Centre foci (Fig. 5) indicate the Outer Centre 2 inclined sheets increase in dip inwards towards Centre 2 (Fig. 5b), supporting Richey and Thomas's (1930) original observations. In contrast, the Centre 1 inclined sheets appear to increase in dip away from the Centre 1 foci (Fig. 5a). This variation in dip implies that the Ardnamurchan inclined sheets are not planar and so cannot be simply extrapolated linearly down-dip to define the source reservoir (cf. Richey and Thomas, 1930; Geldmacher et al., 1998; Burchardt and Gudmundsson, 2009; Siler and Karson, 2009; Tibaldi et al., 2011; Burchardt et al., 2011).

4.2.4. Modes of opening and thickness variations of the inclined sheets

As intrusive sheets are often preferentially emplaced orthogonal to σ_3 (Anderson, 1951), establishing the opening vectors of sheet intrusions therefore determines whether the local stress field conditions active during emplacement promoted development and intrusion of dilatational (mode I) or shear (mode II and III) fractures (Pollard, 1987; Rubin, 1995). Describing the opening vector of the inclined sheets was achieved through correlating marker horizons on either side of inclined sheet intrusions where possible. Field observations are consistent with Keunen's (1937) suggestion that the majority of inclined sheets on Ardnamurchan, regardless of relative dip direction, appear to display dilatational opening vectors. Several inclined sheets exhibit intrusion into shear fractures. For example, in Area 2, one inclined sheet [NM 50618 62002] consists of sinistrally displaced *en échelon* segments, each terminating laterally in a horn (Rickwood, 1990), which is suggestive of mixed mode I and III fracturing resulting in a change in principal stress axes orientations (cf. Pollard, 1987; Rubin, 1995).

Inclined sheet thickness was measured orthogonally to intrusion walls and ranges from 0.05 m to 2.5 m, with an average of 0.6 m. Many sheets with none or only one margin exposed up to 10 m thick were observed (Richey and Thomas, 1930). Fig. 5c highlights an apparent increase in inclined sheet thickness with distance from the Ardnamurchan Central Complex.

5. Anisotropy of magnetic susceptibility (AMS)

Anisotropy of magnetic susceptibility (AMS) detects subtle or weak preferred orientations and alignments of Fe-bearing minerals and reflects the samples fabric (foliation and lineation). To assess the AMS of the inclined sheets, 113 oriented block samples were collected from 69 widely distributed inclined sheets representing examples of all ages, dip dispositions and geometries. For comparison, several ($n = 8$) regional dykes were also analysed. From each block around 10 cm^3 sub-specimens (4–15 per block sample) were prepared according to the procedure described in Stevenson et al. (2007b). Due to the range of inclined sheet thickness and poor exposure, block samples were collected indiscriminately with respect to their position within the sheet. An AGICO KLY-3S Kappabridge was used to measure the magnetic susceptibility of the sub-specimens, which were then averaged for each block sample, assuming they represent a single multi-normal population (Owens, 2000), in order to calculate the block samples magnetic susceptibility tensor. The magnetic susceptibility tensor may be pictured as an ellipsoid with six independent quantities, including three principal susceptibility magnitudes (K_{mean}, H and μ) and a corresponding set of three orthogonal principal axis directions ($K_1 \geq K_2 \geq K_3$). The maximum susceptibility axis (K_1) is the orientation of magnetic lineation and K_3 represents the pole to the magnetic foliation (cf. Owens, 1974; Stevenson et al., 2007b; O'Driscoll et al., 2008). The magnetic susceptibility (K_{mean}), strength of anisotropy (H) and shape of anisotropy (μ) were calculated following Stevenson et al. (2007b):

$$K_{mean} = (K_1 + K_2 + K_3)/3$$

$$H = (K_1 - K_3)/K_{mean}$$

$$L = (K_1 - K_2)/K_{mean}$$

$$F = (K_2 - K_3)/K_{mean}$$

$$m = (K_1 - K_2)/(K_2 - K_3)$$

and

$$\mu = \tan^{-1} m.$$

Plotting L (lineation) against F (foliation) graphically displays the magnetic fabric shape, which is quantified by m, the slope of the line from a point through to the origin, and by μ, the angle from the horizontal axis to the line (Stevenson et al., 2007b). Variation within a block is accounted for by the calculation of 95% confidence ellipses for both the directional and magnitude parameters (Jelínek, 1978).

In this study we equate K_1 to magma flow through correlations to visible magma flow indicators (e.g. Knight and Walker, 1988; Callot et al., 2001; Aubourg et al., 2002; Liss et al., 2002; Horsman et al., 2005; Morgan et al., 2008). Although quantitative image analysis of silicate petrofabrics in thin sections can help to substantiate the correlation between K_1 and magma flow (e.g. Cruden and Launeau, 1994; Archanjo et al., 1995; Launeau and Cruden, 1998), the samples used here are too fine-grained to provide accurate image analyses. Caveats associated with interpreting K_1 as parallel to the magma flow axis are predominantly attributable to variations in magnetic mineralogy or to processes active during intrusion (Tarling and Hrouda, 1993; Geoffroy et al., 2002; Borradaile and Jackson, 2004; Cañón-Tapia, 2004; Cañón-Tapia and Chávez-Álvarez, 2004; Bascou et al., 2005; Philpotts and Philpotts, 2007; Aubourg et al., 2008). Prior to the interpretation of AMS fabrics we therefore conducted high-temperature, low-field magnetic susceptibility experiments and reflected light microscopy to fully characterise the magnetic phase(s) that contribute to the magnetic fraction (Orlický, 1990; Liss et al., 2004). Heating and cooling from 40 °C–680 °C to 40 °C was conducted on powdered samples (see Supplementary Table 2), using a CS-3 furnace attachment for the AGICO KLY-3S Kappabridge, in order to evaluate the magnetic composition. Ferromagnetic (*sensu lato*) minerals (e.g. titanomagnetites) are insensitive to increases in temperature up to the Curie Point (i.e. a sharp decrease in susceptibility), the temperature of which is controlled by the composition of the dominant magnetic phase (Dunlop and Özdemir, 1997). Curie Points were measured using the inflection point or Hopkinson Peak method (Tauxe, 1998; Petrovský and Kapička, 2007).

5.1. Magnetic mineralogy of the inclined sheets

The AMS results (see Supplementary Table 2) from the inclined sheets and regional dykes reveal a range of K_{mean} values from 0.1–23.49 $\times 10^{-2}$ (SI) to 0.05–9 $\times 10^{-2}$ (SI) respectively, consistent with a titanomagnetite carrier of 0.1–10 vol. % (Tarling and Hrouda, 1993). This is corroborated by high-temperature, low-field susceptibility experiments, which suggest that low-Ti titanomagnetites dominate the magnetic mineralogy of the inclined sheets. Hopkinson Peaks are typically absent or suppressed, implying the titanomagnetite grainsize is predominantly multidomain (Liss et al., 2004). The samples analysed in the high-temperature, low-field susceptibility experiments yield a spectrum of results that vary from fully reversible curves with a single Curie Point to more complex irreversible curves with two or more inferred Curie Points. Two typical samples are presented in Fig. 6 (the remainder are contained within Supplementary Fig. 1). On heating, sample CS143 displays a steady increase in susceptibility with temperature until a sharp decrease, correspondent to the Curie Point, at 545 °C (Fig. 6a). Superimposed onto the heating curve is a broad, shallow 'bump' in susceptibility from ~150 to 350 °C (Fig. 6a). This feature, though poorly understood (Hrouda, 2003), is often interpreted to reflect the homogenisation of two exsolved Fe–Ti oxide phases into a single titanomaghaemite phase during the experiment (Özdemir and O'Reilly, 1981, 1982). The amplitude of the 'bump' approximately correlates with the abundance of titanomaghaemite, which in CS143 is minor (Fig. 6a). The Curie Point at 545 °C and the broad peak in susceptibility, at 380 °C, on the cooling curve of CS143 (Fig. 6a) likely indicates a mixture of remnant primary titanomagnetite and secondary (i.e. produced during heating) titanomaghaemite. The Outer Centre 2 inclined sheet sample, CS187, displays a broad peak in susceptibility on heating at ~200–350 °C, likely correlating to titanomaghaemite (Fig. 6b). Compared to CS143, the 'bump' in susceptibility is more readily defined, implying a greater quantity of titanomaghaemite (Fig. 6). The Curie Point at 563 °C on the heating curve (Fig. 6b) is consistent with a low-Ti magnetite phase.

Petrographical observations and reflected light microscopy reveal that titanomagnetite (0.1–0.5 mm), in typical abundances of 3–5 vol. %, dominates the Fe–Ti oxide population of the fine-grained, equigranular dolerites. The Ardnamurchan inclined sheets and regional dykes consist of a cumulus framework of tabular plagioclase and clinopyroxene, occasionally containing olivine, with interstitial quartz and alkali feldspar (Richey and Thomas, 1930). Interstitial titanomagnetites have developed either an elongated or subhedral crystal habit, depending on whether they grew along a boundary between two primary crystals or at crystal triple junctions (e.g. Fig. 7a). Other variable growth forms of titanomagnetite include rare exsolution along plagioclase phenocryst twin planes and skeletal crystals in very fine (~0.1 mm) grained dolerites. There is little evidence of deformation (e.g. fracturing) or post-cumulus modification (e.g. textural equilibration) within the inclined sheets. Therefore, titanomagnetite growth, and likely the magnetic fabric, is controlled by an apparently unmodified primary silicate framework, suggesting a primary magma flow may be inferred (e.g. Callot and Guichet, 2003; Stevenson et al., 2007b).

5.2. Magnetic fabrics of the Ardnamurchan inclined sheets

To independently evaluate the accuracy of the magnetic fabrics record of primary magma flow, a comparison of K_1 orientation and visible field flow indicators was conducted. The long axes of broken

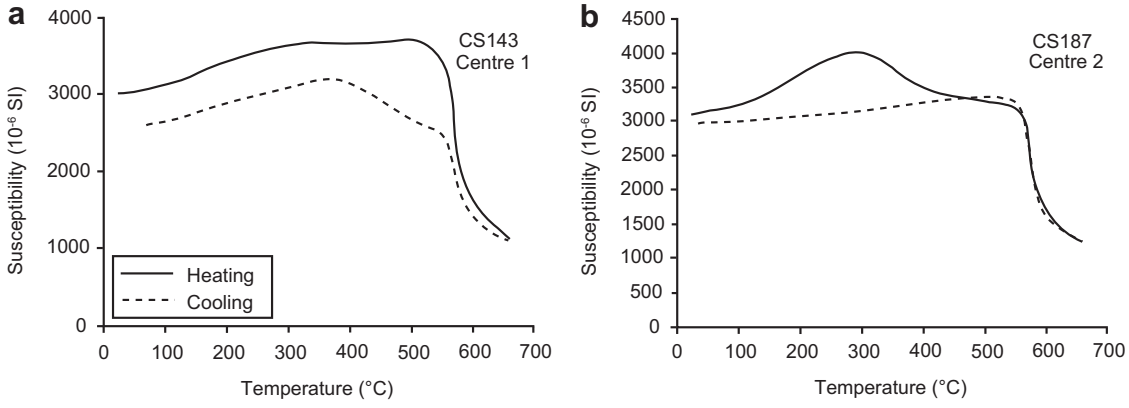

Fig. 6. High-temperature, low-field magnetic susceptibility experiment results. See text for details.

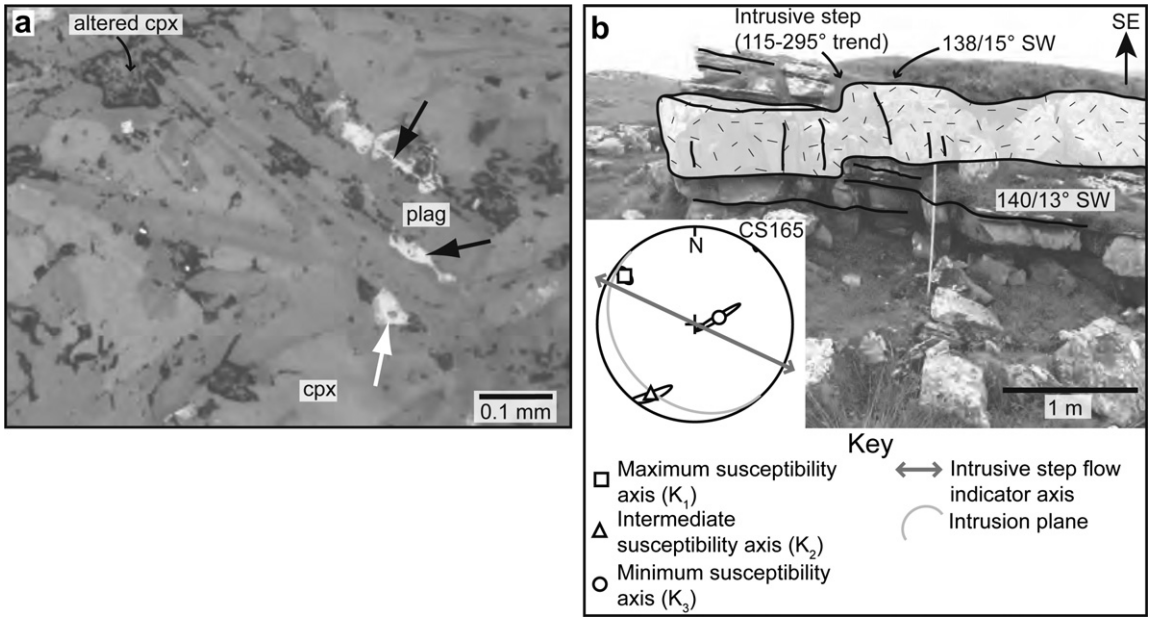

Fig. 7. (a) Reflected light photomicrograph detailing the typical rock microstructures observed in the inclined sheets. Interstitial titanomagnetite is observed to either grow in an elongate fashion along grain boundaries of tabular plagioclase–plagioclase (black arrows) or in a subhedral habit at crystal triple junctions. The long axis of the titanomagnetite importantly is often parallel to that of the primary silicates. (b) Sill section of an inclined sheet, from Area 1, with an intrusive step [NM 49263 62683]. The K_1 lineation, interpreted as equivalent to the primary magma flow axis, is sub-parallel to the intrusive step axis.

bridge and intrusive step structures or flow lines on intrusive sheet walls may be used in the field to approximate the primary magma flow axis (Rickwood, 1990; Correa-Gomes et al., 2001; Liss et al., 2002; Hutton, 2009; Schofield et al., 2012). Several locations on Ardnamurchan provided sufficient constraints on magma flow to test the magnetic data. Fig. 7b highlights an example of the AMS fabric correlated to a measured field flow indicator. Comparison between the visible field flow indicator axes and K_1, of 16 inclined sheets and two regional dykes, reveals 72% of the K_1 lineation azimuths are within 30° (i.e. to either side) of the measured field flow axes. It is probable that the ambiguity associated with measurement of visible field flow axes has contributed to this error. The broad correlation to visible field flow indicators further suggests the magnetic lineation correlates to the primary magma flow axis (Correa-Gomes et al., 2001; Liss et al., 2002).

The preponderance of prolate fabrics means that magnetic foliations are not as well defined as the magnetic lineation (Supplementary Table 2) and therefore not so reliable. In total, 66 inclined sheets (106 samples) are represented in the magnetic lineation analysis and the results displayed on a simplified geological map of Ardnamurchan (Fig. 8a; see Supplementary Fig. 2 for sample locations and raw AMS data). Seven AMS samples (see Supplementary Table 2) proved unusable for magnetic lineation interpretation as the K_1 and K_2 confidence ellipses overlapped, implying the magnetic fabric only has a planar component (i.e. no lineation may be derived). Magma flow axes inferred from previous inclined sheet emplacement models suggest K_1 plunge azimuths should predominantly radiate up and out from the central source (Palmer et al., 2007). Fig. 8a displays a map of all magnetic lineations, from which no definitive radial trend may be described. Extrapolating the K_1 axes along the plunge azimuth (i.e. regardless of plunge direction) indicates that, whilst the majority (73%) intersect the Ardnamurchan Central Complex, 27% ($n = 29$) of magnetic lineations are oriented tangentially to the central complex margins (Fig. 8a). These tangential magnetic lineations are more abundant to the east and north-east of the Ardnamurchan Central Complex (Fig. 8a). Out of the K_1 axes that may be traced into the central complex, many do not correlate to the specific Centre foci defined by Richey and Thomas (1930). Overall, a dominant NW–SE trend is apparent in the Ardnamurchan inclined sheets, similar to that observed in the regional dyke K_1 azimuths (Fig. 8b).

Magnetic lineation plunges range from 0° to 82°. An equal-area, lower-hemisphere stereographic projection of the K_1 vectors indicate that 70% of samples exhibit plunges ranging from sub-horizontal (0–20°; $n = 40$) to moderate (≤45°; $n = 33$) (Fig. 8c). The remaining 30% ($n = 30$) of the magnetic lineations are steeper (≥45°) (Fig. 8c). Accounting for samples collected from the same intrusion, 38 inclined sheets contain purely sub-horizontal to moderate plunges and 17 inclined sheets contain steep plunges (≥45°). Seven inclined sheets, displaying a ramp-flat morphology, contain both shallow and steep K_1 plunges measured from separate block samples. Magnetic lineations within the regional dykes are generally moderately inclined (42° mean) but range from 10° to 77° (Fig. 8c).

Fig. 9a displays a plot of K_1 plunge azimuth against inclined sheet dip azimuth and inclined sheet strike. Fig. 9a indicates there is little correlation observed between K_1 plunge azimuth and inclined sheet dip azimuth, with only 12 inclined sheets (16 samples) containing a K_1 plunge azimuth within 30° of the dip azimuth (Fig. 9a). With respect to the Ardnamurchan Central Complex, these 12 inclined sheets are variably distributed (Fig. 9a) to the SE ($n = 6$), S ($n = 3$), N ($n = 1$), NE ($n = 1$) and within the Centre 3 inclined sheet swarm ($n = 1$). Instead, a greater positive correlation is observed between inclined sheet strike and K_1 azimuth (corrected to a value <180° by removing the plunge direction) (Fig. 9b). Twenty inclined sheets (21 samples), widely distributed throughout Ardnamurchan, contain a K_1 azimuth within 30° of the inclined sheet strike. The plunge of these tangential lineations ranges from 0° to 66°. The majority of inclined sheets appear to display no correlation between K_1 and inclined sheet orientation, suggesting oblique magma flow was dominant. There is also little correlation between the magnetic foliation and inclined sheet orientation; although this likely reflects the dominance of prolate fabrics and variations in block sample position

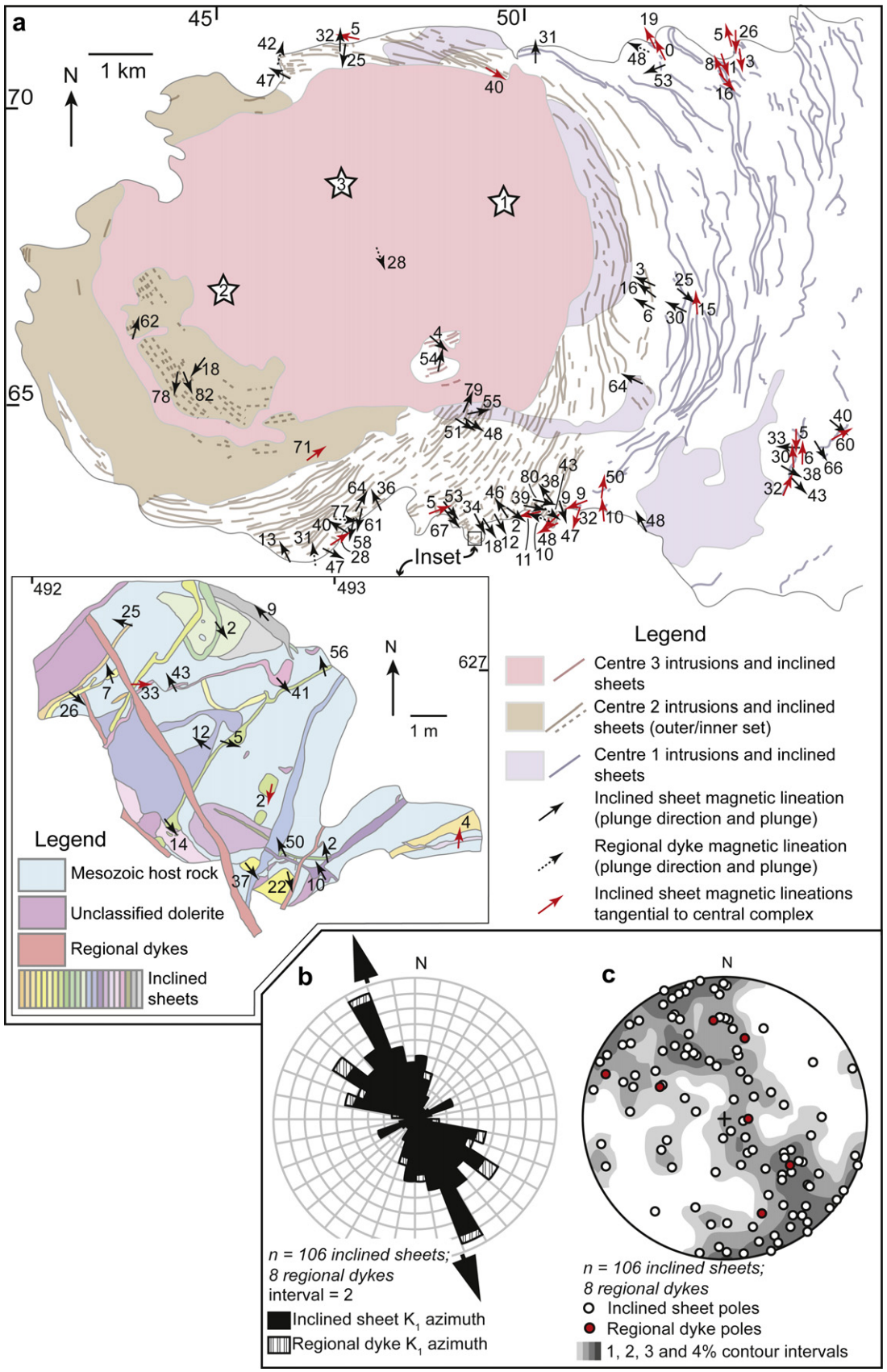

Fig. 8. (a) Map of the Ardnamurchan inclined sheets and the magnetic lineations (b) Rose diagram of all K_1 axes, with a strong NW–SE trend. (c) Equal-area stereographic projection of K_1 lineations showing a NW–SE trend and preponderance of sub-horizontal to moderately inclined plunges.

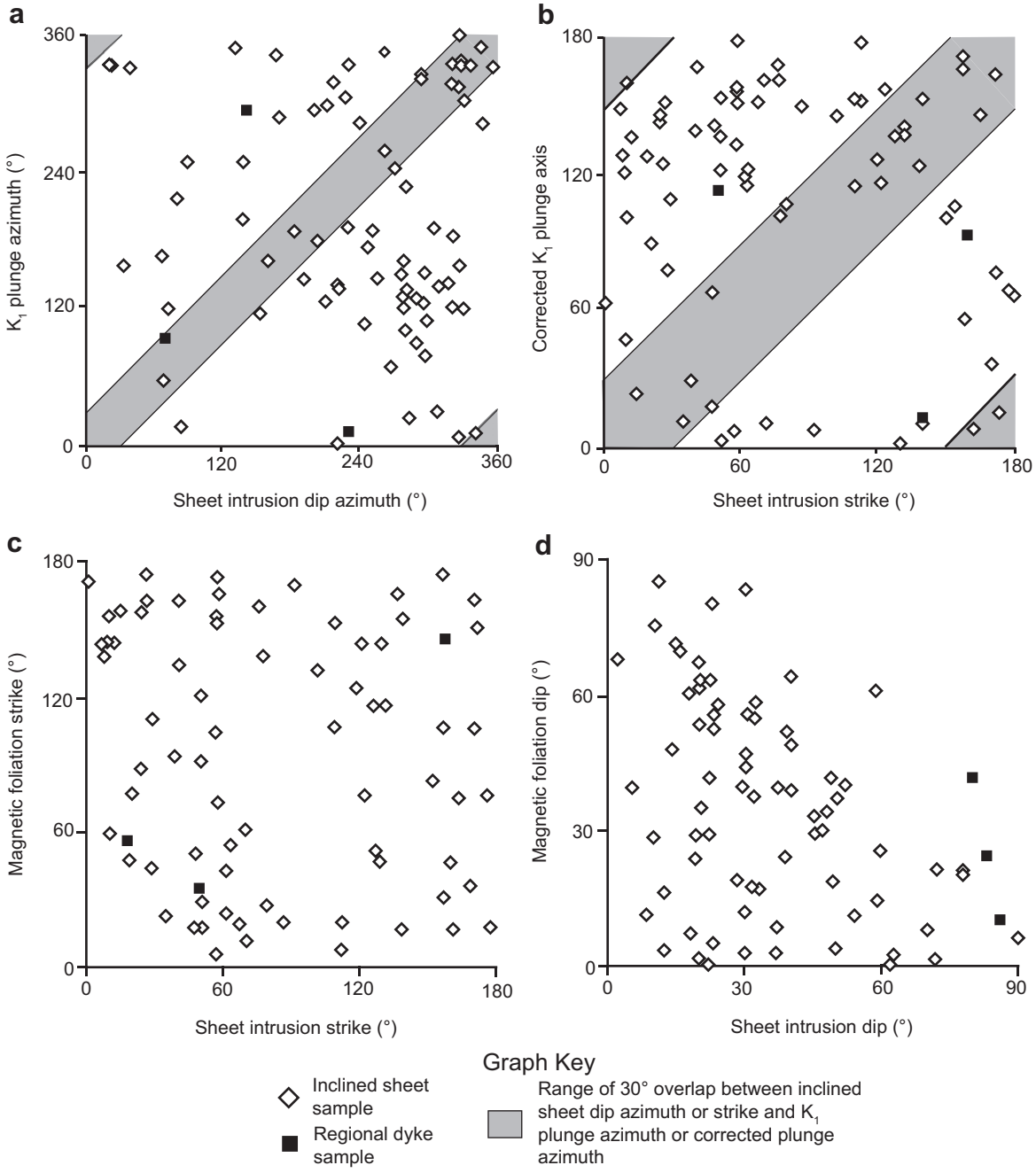

Fig. 9. (a) and (b) Graphs highlighting the weak correlation between K_1 azimuth and inclined sheet dip azimuth and strike. The corrected K_1 azimuths, for correlation with inclined sheet strike, ignore plunge direction and were converted to $<180^\circ$ if required. (c) and (d) Plots showing the lack of relationship between the magnetic foliation and the orientation of the inclined sheets.

relative to sheet margins rather than perturbations in primary magma flow trends. Importantly, K_1 remains consistently oriented regardless of K_3 variations. In one of the seminal studies applying AMS to determining magma flow in sheet intrusions, Khan (1962) measured several samples from the Ardnamurchan inclined sheets, highlighting that the K_1 axes are located within the dyke plane and are oriented at a moderate angle to sheet dip; corroborating the magnetic lineation relationships described in this study.

6. Emplacement of the Ardnamurchan inclined sheets

Previous models for 'cone sheet' emplacement (e.g. Anderson, 1936; Phillips, 1974; Walker, 1993; Schirnick et al., 1999) are based almost exclusively on the following criteria: 1) inclined sheet strike should be roughly concentric; 2) all inclined sheets dip inwards to a common magma source; 3) magma flow always radiates upwards and outwards from the central source reservoir.

Our results from the Ardnamurchan inclined sheets indicate: 1) strikes are roughly concentric close to the central complex but appear weakly deflected, from a NW–SE trend, around the central complex further away; 2) inclined sheet dip values and azimuths are highly variable (e.g. outward-dipping) and often cannot be traced back to the respective Centre foci; 3) there is a greater abundance of inclined sheets to the SE of the central complex; 4) primary magmatic flow indicators (within error) and AMS fabrics in the inclined sheets are consistently oriented NW–SE with

predominantly sub-horizontal to moderate plunges. While there is some similarity between these observations and the predictions of previous emplacement models, significant variations (e.g. in inclined sheet dip) exist. Here, we attempt to reconcile earlier emplacement models with features of the Ardnamurchan inclined sheets that have been previously overlooked.

6.1. Controls on inclined sheet intrusion

6.1.1. The role of pre-existing host rock structures

The geometries and orientations of inclined sheets have traditionally been attributed to the morphology of a compressive local stress field surrounding an expanding centralised magma source, where σ_1 is radially inclined inwards and σ_3 is oriented parallel to the margins of the central source (e.g. Anderson, 1936; Durrance, 1967; Gautneb et al., 1989; Gautneb and Gudmundsson, 1992; Schirnick et al., 1999; Geshi, 2005; Burchardt et al., 2011; Tibaldi et al., 2011). Recent field (e.g. Burchardt, 2008; Schofield et al., 2010) and experimental (e.g. Gudmundsson, 1998, 2006; Kavanagh et al., 2006; Menand, 2008) studies have shown that pre-existing host rock structures and lithologies may also significantly control sheet emplacement. Although a few studies of inclined sheets allude to the affects of the host rock on intrusion distribution and form (e.g. Gudmundsson, 2002; Burchardt, 2008; Siler and Karson, 2009), a detailed consideration of potential host rock controls may aid our understanding of local inclined sheet variations that are often overlooked (Klausen, 2004). Determining the influence of host rock controls on intrusion geometry may also allow the morphology of the contemporaneous stress field to be refined (Jolly and Sanderson, 1997).

Field observations reveal that emplacement of the Ardnamurchan inclined sheets was primarily facilitated by brittle deformation of the host rock. The geometry and orientations of the inclined sheets can therefore be used to infer the stress field active during emplacement (Delaney et al., 1986; Rubin, 1995; Jolly and Sanderson, 1997; Schofield et al., 2012). Sheet intrusions are often considered to generate and intrude new fractures orthogonal to σ_3 (Anderson, 1951). However, the wide distribution of inclined sheet orientations and the observation that some inclined sheets are sub-parallel to outward-dipping bedding planes (Day, 1989) and then abruptly transgress up through stratigraphy parallel to inwardly inclined, moderately-dipping fractures suggests that contemporaneous intrusion along pre-existing host rock anisotropies oblique to σ_3 occurred (McKeagney et al., 2004). These two principal orientations of the Ardnamurchan inclined sheets are approximately conjugate, the orientation of which defines an average radial, inwardly inclined σ_1 with respect to the central complex (Fig. 10a; Day, 1989). The principal stress axes orientations in Fig. 10a are typical of local compression, congruent with the development of synchronous thrust faults (Day, 1989). In contrast, resolved principal stress axes for the conjugate fracture set highlight formation in an extensional stress regime, with σ_1 sub-vertical and σ_3 horizontal (Fig. 4c). Conjugate fracture formation may therefore relate to regional extension and/or to periods of local extension associated with major intrusion deflation (cf. Day, 1989), prior to inclined sheet intrusion. Observed chilled margins of some inclined sheets against outward-dipping fracture planes supports this hypothesis. Although these pre-existing inward-dipping fractures and outward-dipping bedding or cleavage plane anisotropies may have been annealed during contact metamorphism associated with intrusion of the Hypersthene Gabbro (Day, 1989), they would still represent planes of lower cohesive strength (i.e. easier for sheet intrusions to intrude) compared to the intact host rock.

Having established that pre-existing host rock anisotropies were likely preferentially exploited during inclined sheet intrusion, it is

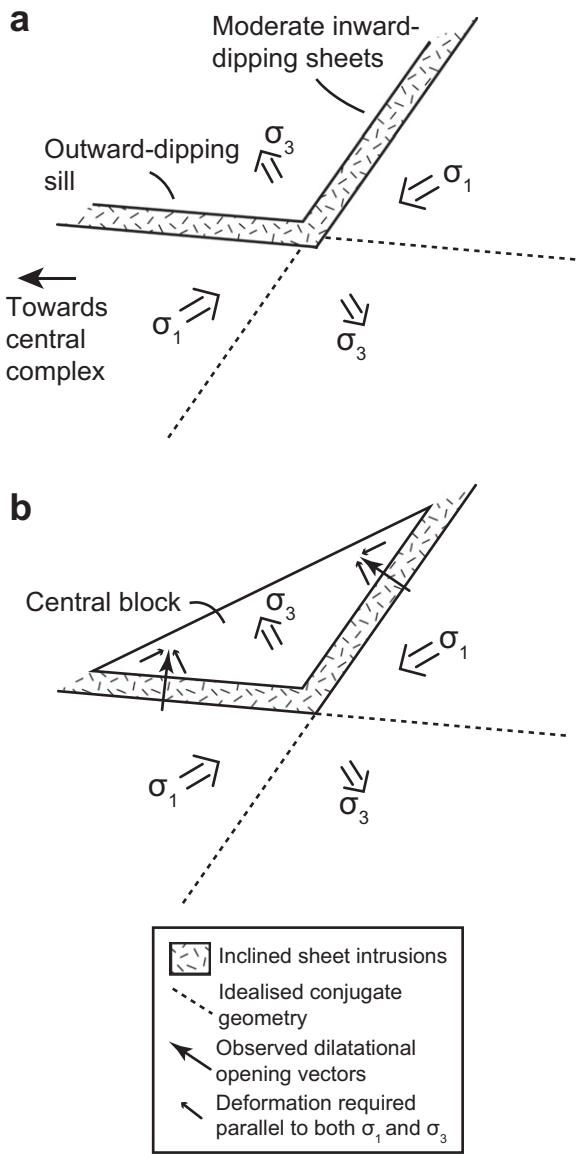

Fig. 10. Schematic cross-sections of the (a) conjugate nature of the outward- and inward-dipping inclined sheet segments defining an inwardly inclined σ_1 principal stress axis. (b) Highlights the required deformation of an uplifted central block given the dilatational opening vectors of the inclined sheets.

apparent that the active stress field was suitably oriented to promote fracture or bedding plane reactivation. This preference to exploit two specifically oriented pre-existing anisotropies may also explain the clustering of the inclined sheet poles into two apparently separate populations (Fig. 2), despite field relationships (e.g. ramp-flat morphologies) indicating that the inclined sheets are contemporaneous. The methodology of Jolly and Sanderson (1997) can therefore be applied to further refine the position of the principal stress axes for individual areas, based on the distribution of all the inclined sheet poles and the preponderance of dilatational opening vectors (i.e. parallel to σ_3). Fig. 4b and c depicts a worked example from Area 1 (Fig. 2). The principal eigenvector of the gross cluster of the inclined sheet poles, located within an ellipse encompassing the poles, represents σ_3 (128/73°; Fig. 4c). A plane bisecting the ellipse, through its long axis, and σ_3 is taken to represent the σ_2–σ_3 plane, as fracture opening is easier closer to σ_2 than σ_1 (Fig. 4c; Jolly and Sanderson, 1997; McKeagney et al., 2004).

The pole to the σ_2–σ_3 plane is equivalent to σ_1 (308/17°; Fig. 4c). The calculated principal stress axes for all areas are displayed in Fig. 2 and confirm that σ_1 was radially inclined inwards (increasing in plunge towards the central complex) and σ_3 was steeply to moderately outwardly inclined. This may explain why the outward-dipping fractures, of the conjugate fracture set, were not intruded; i.e. their orientation is approximately orthogonal to a radially inwardly inclined σ_1 (Fig. 10a).

A comparison between the defined axes of σ_3 and the wide range of inclined sheet poles implies that many inclined sheets should display opening vectors with a shear displacement, as the majority of orientations is not purely orthogonal to σ_3. However, many inclined sheets are observed to have dilated, implying that both vertical (i.e. uplift) and horizontal displacement of the central block occurred (Fig. 10b). Because the sheets are inclined and have an overall concentric strike, this requires a reduction in volume of the uplifted central block (Fig. 10b). On Ardnamurchan, observed bedding-parallel stylolites and recrystallised host rock textures (Day, 1989) may provide evidence of internal deformation and porosity reduction corresponding to the diminution of the central block volume. It is also plausible that host rock anisotropies ahead of the propagating magma tip were reactivated originally as shear fractures but providing the internal magma pressure of an intrusion exceeds the compressive stress orthogonal to the intrusive plane, dilatational opening should still dominate (i.e. in compressive stress regimes).

6.1.2. Evolution of the Ardnamurchan Central Complex inclined sheet swarms

Local stress fields associated with magma chambers vary temporally and are controlled by the shape, depth and internal pressure of the source reservoir (Gudmundsson, 1998). Mathieu et al. (2008) suggested inclined sheet intrusion on Ardnamurchan was related to the intrusion and inflation of a sill into a laccolith, which instigated host rock doming and fracturing. The stress regime highlighted here by the analysis of the inclined sheets is consistent with the expansion of a central laccolith (cf. Jackson and Pollard, 1988; Schirnick et al., 1999). Doming of the host rock associated with the laccolith expansion is constrained to a belt of country rock coincident to the lateral margins of the intrusion (Pollard and Johnson, 1973; Jackson and Pollard, 1988) and results in two zones of flexure where contraction and extension occurs (Pollard and Johnson, 1973). Within the BIPIP, including Ardnamurchan, inclined sheet swarms are spatially restricted to concentric belts coincident with zones of intrusion-induced flexure (Walker, 1975). It is likely that extensional conjugate fractures, developed in areas of flexure, and bedding planes were rotated during doming to angles that relative to the local principal stress axes promoted reactivation and intrusion (Fig. 11). Fig. 11 highlights that inclined sheets close to the laccolith may exploit moderate to steep inward-dipping fractures whilst with distance away from the central complex the proportion of bedding planes that may be intruded increases. The steepening inwards trend of the Ardnamurchan Centre 2 inclined sheet set and the Loch Scridain sill-complex on Mull, which is likely genetically associated to the Mull inclined sheets (Kerr et al., 1999; Emeleus and Bell, 2005), may support this scenario.

There is a wide variation in inclined sheet orientation on a local scale, manifested as complex cross-cutting relationships. Subtle fluctuations in the orientation of the local principal stress axes may account for this. Many major intrusions (e.g. laccoliths) are recognised as having assembled from discrete magma pulses emplaced incrementally (Pitcher, 1979; Glazner et al., 2004; Stevenson et al., 2007a; Zellmer and Annen, 2008; Annen, 2009), which promotes cyclical magma chamber inflation and deflation. On Ardnamurchan, field relationships suggest the intrusion of inclined sheets, and formation of associated thrust faults, occurred intermittently with the formation of normal faults (Day, 1989). This supports the occurrence of temporal fluctuations of the active stress field between localised compressional and extensional regimes (Day, 1989; Mathieu and van Wyk de Vries, 2009).

6.2. Magma flow pattern and magma source position

We suggest that the magnetic lineations measured from the inclined sheets reflect the primary magma flow pattern because: 1) they are overall consistently oriented NW–SE; 2) the fabrics are dominantly prolate (i.e. typical of a flow fabric; Horsman et al., 2005); 3) there is a strong correlation between magma flow axes inferred from visible field flow indicators and K_1; 4) there is little to no evidence of post-emplacement deformation; and 5) the K_3 axes would be consistently oriented if an ambient tectonic strain field was recorded.

Magma within centrally fed inclined sheets is expected to have flowed radially upwards and outwards (Palmer et al., 2007), implying that the measured magma flow axes (e.g. magnetic lineations) should correlate to the respective inclined sheet dip azimuth and dip angle. This relationship may be observed in the Otoge igneous centre (Japan), where magma flow indicators (e.g. vesicle imbrication) are sub-parallel to centrally fed inclined sheet dips (from a geochemically determined source) (Geshi, 2005). However, out of the 69 Ardnamurchan inclined sheets analysed for AMS, only 12 inclined sheets contain magnetic lineations that are sub-parallel to the inclined sheet dip angle and dip azimuth (Fig. 9a). Instead,

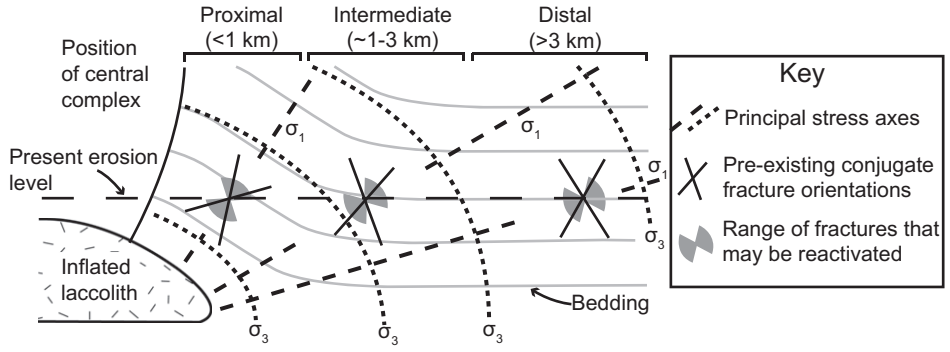

Fig. 11. Sketch of local principal axes orientations formed in response to an inflating laccolith and the resultant fracture/bedding planes that are reactivated. Proximal to the laccolith only steep fractures are reactivated and at an intermediate distance, where most of the Ardnamurchan inclined sheets are situated, intrusion exploits both moderate inward-dipping fractures and bedding planes. Distally, bedding planes are predominantly intruded.

the majority of the Ardnamurchan inclined sheets (73%) contain AMS fabrics suggestive of a lateral magma flow pattern. Although the restricted lateral extent of the inclined sheets potentially limits lateral magma flow, this may be an artefact of poor exposure or may signify sub-surface intrusive offsets (cf. Gudmundsson, 2002; Macdonald et al., 1988, 2009). Magma flow from one segment to another in this latter hypothesis may partially explain the local variations observed in the K_1 axes. However, it is the consistency in orientation of locally adjacent magnetic lineations, often measured from separate sheets, that importantly suggests a significant proportion lateral magma flow. Two mechanisms, potential complimentary, are considered that may explain the observed magma flow pattern.

6.2.1. Centrally fed inclined sheets

To maintain a central source and explain the preponderance of NW–SE magnetic lineations, magma flow parallel to inclined sheet dip (*sensu* Anderson, 1936) may have been geographically restricted to the NW and SE of the Ardnamurchan Central Complex (Fig. 12a). Continued intrusion of magma into the inclined sheets may then promote lateral propagation concentrically around the central complex, following the local compressive σ_3 trajectory, if vertical propagation was inhibited by sheet arrest (cf. Gudmundsson, 2002) or the rate of intrusion exceeded an eruption rate (i.e. assuming the inclined sheets breached the surface). This phase of lateral magma flow, predominantly to the NE and SW of the Ardnamurchan Central Complex, would augment the observed NW–SE magnetic lineation trend (Fig. 12a). Implicitly, magnetic lineations sub-parallel to inclined sheet dip should be primarily located to the SE of the Ardnamurchan Central Complex (there is no exposure to the NW). Although 50% ($n = 6$) of inclined sheets containing dip-parallel magnetic lineations are distributed to the SE of the Ardnamurchan Central Complex, this is a relatively minor quantity considering 27 adjacent inclined sheets display evidence of lateral magma flow. This disparity may potentially be explained if inclined sheet dip-parallel magnetic lineations are overprinted by secondary lateral magma flow (cf. Tauxe et al., 1998; Philpotts and Philpotts, 2007).

6.2.2. An alternative emplacement model

From the strike and magma flow patterns of the inclined sheets, a series of traces deflected around the Ardnamurchan Central Complex, from an original NW–SE trend, may be interpreted (Fig. 12b). This is particularly evident in the inclined sheets furthest from the central complex. A novel alternative to centrally fed inclined sheets is that the sheets may have intruded from a laterally

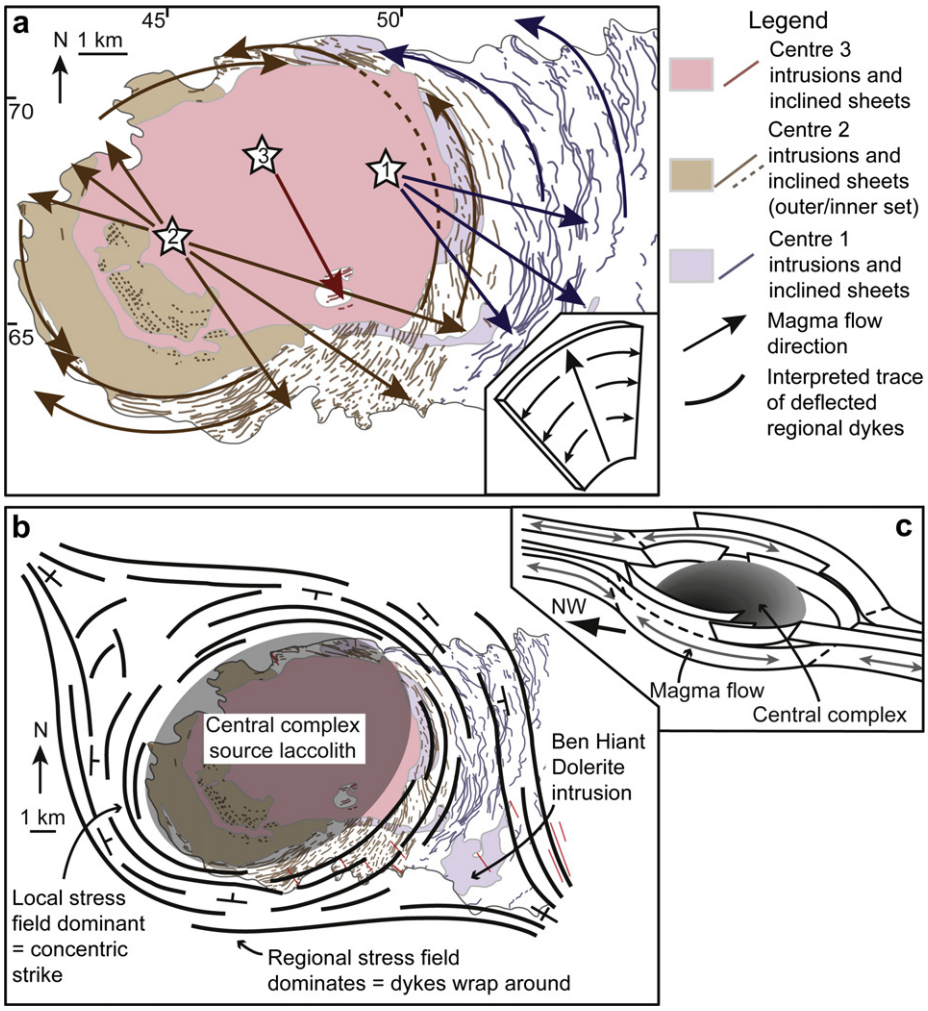

Fig. 12. (a) Expected magma flow pattern, consistent with the observed magnetic lineations, if the inclined sheets were fed from a central source. Magma is fed up-dip to the SE and/or NW of the central source and then begins to propagate laterally and concentrically around the central complex (see inset). (b) Map of Ardnamurchan depicting the general and interpreted inclined sheet and regional dyke strikes and the approximate lithostatic stress zones defined by stress field interference. (c) Conceptual model of 'cone-sheets' representing an inclined form of laterally propagating regional dyke.

adjacent source, independent of the Ardnamurchan Central Complex. The dominant areas of upper crustal magma genesis in the BIPIP, the central complexes, are often interconnected by numerous regional dykes (Emeleus and Bell, 2005). For example, Speight et al. (1982) identified over 300 regional dyke outcrops between the Mull and Ardnamurchan Central Complexes. On Ardnamurchan, the NW–SE magnetic lineation trend (150–330°) of the inclined sheets is virtually indistinguishable from the local strike (160–340°; Speight et al., 1982) and lateral magma flow patterns (138–318°; this study) of the regional dykes, suggestive of a common origin. It is proposed that laterally propagating regional dykes, fed from one or more central complexes, were deflected into a 'cone sheet-like' geometry upon entering and interacting with the Ardnamurchan Central Complex (Fig. 12b).

Evidence of lateral magma flow in the regional dykes is widespread throughout the BIPIP (e.g. Herrero-Bervera et al., 2001) and is supported by the convergence of dyke strikes on central complexes (Odé, 1957; Klausen, 2006). Macdonald et al. (1988, 2009) and Wall et al. (2009) showed that regional dykes in NE England and the southern North Sea, respectively, were likely originated from the Mull Central Complex located >400 km to the NW. Several studies of other volcanic systems preserved throughout the geological record in Canada (Ernst and Baragar, 1992; Ernst et al., 1995), Argentina (White, 1992), the Galapagos Islands (Geist et al., 1999), Hawaii (Rhodes et al., 1989) and Ethiopia (Grandin et al., 2009, 2011) support lateral magma transport within extensive dykes as a mechanism for feeding distal (20–2000 km distant) intrusions and/or extrusions. However, the source(s) of the regional dykes remains uncertain. Pinel and Jaupart (2004) calculated that horizontal dyke propagation is preferentially instigated beneath large volcanic edifices. Compared to the Ardnamurchan Central Complex, the Mull and Skye Central Complexes (both similar in size) are significantly larger (Bott and Tuson, 1973) and may be potential regional dyke sources.

Crucial to the model of a regional dyke origin for the Ardnamurchan inclined sheets is the operation of a mechanism to deflect the sub-vertical, NW–SE trending regional dykes into an inverted conical geometry. Within the regional dyke swarm associated with the Mull Central Complex, Jolly and Sanderson (1995) observed an increase in the range of dyke orientation with proximity to the source, which they attributed to the affect of the local stress field. Similarly, it may be envisaged that regional dykes propagating laterally into the local stress field of the Ardnamurchan Central Complex were reoriented to maintain a plane of intrusion orthogonal to σ_3 (cf. Anderson, 1951; Pollard and Johnson, 1973; England, 1988; Klausen, 2006). While inclined sheet dip was controlled by the intrusion of pre-existing anisotropies, the strike of each inclined sheet was likely dependent on the transition and interference between the local and regional stress fields. Proximal to the Ardnamurchan Central Complex, where the local stress field was dominant (i.e. during local compression), there is a preponderance of concentric, inclined sheets (Fig. 12b). However, with distance from the central complex the magnitude of the local stress field decreases (Gautneb and Gudmundsson, 1992) and inclined sheet strikes may only be weakly deflected from the regional NW–SE trend (Fig. 12b). Beyond the influence of the local stress field, sub-vertical, NW–SE striking regional dykes would be formed (Speight et al., 1982; England, 1988). This gradual transition between concentric, inclined sheets to regional dykes may explain the increase in dip of the Centre 1 inclined sheets with distance from the Ardnamurchan Central Complex.

6.2.3. Source of the Ardnamurchan inclined sheets

Given that magnetic lineations sub-parallel to both inclined sheet dip (i.e. in support of a central source) and strike (i.e. perhaps more applicable to a regional dyke source) are observed, it is likely that both mechanisms occurred. However, the preponderance of lateral magma flow patterns throughout the Ardnamurchan inclined sheets suggests that centrally fed sheets had a significantly lower intrusive volume compared to the proposed laterally propagating regional dykes. This may imply that centrally fed sheets had a reduced magma supply or that their injection was temporally restricted. For sheet intrusion from a central magma chamber to occur, the magmatic overpressure must exceed the minimum principal stress and tensile strength of the wall rock and the mechanical properties of the heterogeneous host rock must allow magma propagation (Gautneb and Gudmundsson, 1992; Gudmundsson and Phillip, 2006). There are two processes which may inhibit centralised inclined sheet intrusion. Firstly, magmatic overpressure may not necessarily be accommodated by sheet intrusion (Gautneb and Gudmundsson, 1992) as is often assumed, but can also be reduced by magma chamber growth instead (Schirnick et al., 1999). Secondly, significant mechanical variation in the host rock within the close vicinity of the magma chamber may promote sheet arrest until stress field homogenisation occurs (Gudmundsson and Phillip, 2006). Either of these processes, or a combination of both, may have acted to restrict inclined sheet intrusion from the Ardnamurchan Central Complex.

6.2.4. Differentiating between the two proposed emplacement models

Without detailed magma flow analyses of inclined sheets, it may be difficult to differentiate between centrally fed and potential laterally fed inclined intrusions. Here, we discuss two methods, independent of magma flow analysis, applied to Ardnamurchan that may provide a proxy of magma source position.

Firstly, inclined sheets are often more abundant in geographical areas containing the intersection between the central complex and either the contemporaneous, regional σ_1 axis (e.g. Ardnamurchan, Richey and Thomas, 1930; Skye, Walker, 1993) or the regional σ_3 axis (e.g. La Gomera, Canary Islands, Ancochea et al., 2003; Otoge, Japan, Geshi, 2005) principal stress axes. It is suggested that this relationship may be attributed to the influence of the regional stress field during emplacement. Dilatational opening of inclined sheets requires both uplift and crustal extension, which assuming intrusion orthogonal to the σ_3 axis occurs (Anderson, 1951), suggests centrally fed inclined sheets should preferentially intrude in a direction equivalent to the regional σ_3 axis, so that their strike is parallel to σ_1. This is supported by the distribution of the centrally sourced inclined sheets predominantly to the E and W of the Otoge igneous complex (Japan) as emplacement was coeval to E–W regional extension (Geshi, 2005). In contrast, lateral propagation of regional dykes towards, and deflected around, a central complex should result in the concentration of inclined sheets in one or both geographical sectors that contain the intersection between the regional σ_1 or σ_2 axis (depending on which is sub-horizontal) and the central complex. Throughout the evolution of the BIPIP, σ_3 was oriented NE–SW, as indicated by the NW–SE strike of the regional dyke swarms (Speight et al., 1982; England, 1988). Given the regional σ_3 axis orientation, inclined sheets derived from a central source should therefore be more abundant to the NE and SW of the Ardnamurchan Central Complex. However, the Ardnamurchan inclined sheets appear more abundant to the SE of the central complex (the NW quadrant is offshore). The observed distribution and abundance of the Ardnamurchan inclined sheets, in quadrants containing the regional σ_1–central complex intersection (i.e. SE), therefore does not conform to the expected distribution for centrally fed inclined sheets but supports a regional dyke origin.

A further important distinction between centrally fed and laterally fed inclined sheets is the implicit difference in

geochemical characteristics expected. The BIPIP regional dykes are lithologically diverse, though broad spatially controlled groupings, corresponding to proximity to specific central complexes, are observed (Emeleus and Bell, 2005). For example, the dyke swarm in the region surrounding the Mull Central Complex is typically associated with tholeiitic basalts and, locally, alkali-olivine dolerites (Emeleus and Bell, 2005), though localised major and trace element compositional variation exists (cf. Kerr et al., 1999). In contrast, the regional dykes associated with the Skye Central Complexes are significantly more compositionally diverse, with ultrabasic-to-silicic lithologies reported (Emeleus and Bell, 2005). A detailed comparison between the Ardnamurchan inclined sheets and the broad regional dyke swarm is beyond the scope of this study, at least in part due to the large range in chemical composition observed (Emeleus and Bell, 2005). However, the comprehensive geochemical and isotopic study of Geldmacher et al. (1998) on the Ardnamurchan inclined sheets makes several pertinent observations possible. Tholeiitic basalts also dominate the inclined sheet lithologies on Ardnamurchan, with major and trace element geochemistry allowing the distinction of high (>4.6 wt.%) and low (<4.6 wt.%) MgO types; these sub-groups are also distinguishable based on their $^{87}Sr/^{86}Sr$ and $^{143}Nd/^{144}Nd$ isotopic compositions. Geldmacher et al. (1998) found no compositional distinction between the inclined sheet populations of the purported different centres of activity, and suggested that the compositional variation observed reflected varying amounts of fractionation and interaction with Archean (Lewisian) basement gneisses and Neoproterozoic (Moinian) metasedimentary rocks. Geldmacher et al. (1998) also showed that the Ardnamurchan inclined sheets with >4.6 wt.% MgO exhibit overlap with the Mull plateau basalt compositions with respect to initial $^{143}Nd/^{144}Nd$ isotopic composition. In addition, Kerr et al. (1999) recognised three sub-groups of 'cone-sheets' associated with the Mull Central Complex, with initial $^{87}Sr/^{86}Sr$ and $^{143}Nd/^{144}Nd$ compositions ranging between 0.70464–0.71822 and 0.51190–0.51279, respectively (their Table 4). Importantly, the range of initial (60 Ma) $^{87}Sr/^{86}Sr$ and $^{143}Nd/^{144}Nd$ isotopic compositions of 0.70528–0.74234 and 0.51185–0.51220, respectively, reported by Geldmacher et al. (1998) for the Ardnamurchan inclined sheets overlaps significantly with the data of Kerr et al. (1999). In the absence of a detailed geochemical and isotopic study of the Mull regional dyke swarm, we take this as permissible evidence that the Mull magmatic system may have sourced the Ardnamurchan inclined sheets.

6.3. Implications of emplacement mechanism to edifice construction

Volcanic edifice construction is often assumed to result purely from intrusive activity related to a vertically stacked magmatic system with an upper crustal magma chamber (Acocella and Neri, 2009). Inclined sheets are major constituents of the sub-volcanic intrusive framework of many igneous centres preserved throughout the geological record. Whilst there are good examples of centrally fed inclined sheets intrusions (e.g. the Otoge inclined sheets, Japan Geshi, 2005; the Stardalur inclined sheets, Iceland, Tibaldi and Pasquarè, 2008), our results suggest that volcanic edifice construction may not be dominantly vertical, but that adjacent or regional magmatic systems could contribute in a significant way.

Lateral emplacement of inclined sheets, as proposed here, requires a series of adjacent volcanic complexes interconnected by magmatic pathways, such as regional dykes, with sub-horizontal magma flow regimes. This may be satisfied in areas associated with rifting events as volcanism is often manifested as a series of potentially interlinked central complexes and regional dyke swarms (e.g. Iceland, Siler and Karson, 2009; BIPIP, Emeleus and Bell, 2005; Canary Islands, Schirnick et al., 1999; Gudmundsson, 2002; Afar, Grandin et al., 2009). Similar to the BIPIP, many regional dyke swarms in Iceland, the Canary Islands and the Afar contain evidence of lateral magma flow (e.g. Marinoni and Gudmundsson, 2000; Paquet et al., 2007; Grandin et al., 2009) and are observed to focus on, and become more intense towards central complexes (e.g. Teno massif, Tenerife, Marinoni and Gudmundsson, 2000; Birnudalstindur igneous centre, Iceland, Klausen, 2006). Laterally propagating regional dykes in these volcanotectonic settings similar to Ardnamurchan may therefore interact with and possibly deflect around (i.e. inclined sheets) central complexes. This may explain the low abundance of regional dykes, compared to inclined sheets, often documented within the central complexes (Schirnick et al., 1999; Siler and Karson, 2009).

7. Conclusions

Sub-volcanic intrusion, of which inclined sheets are a major constituent, partially controls the growth and eruptive style of volcanic edifices. Locally variable inclined sheet geometries and a consistent NW–SE trending, sub-horizontal to moderately plunging magma flow pattern observed within the archetypal inclined sheets around the Ardnamurchan Central Complex do not fully conform to previous emplacement models. Several insights may be elucidated from this study, which suggest our current understanding of inclined sheet emplacement may be oversimplified.

1. Inclined sheets may be fed laterally from adjacent volcanic centres via regional dykes. On Ardnamurchan, magma flow data suggests contemporaneously intruded inclined sheets were fed from both lateral (~73%) and central (~27%) sources. The laterally propagating regional dykes likely originated from the Mull Central Complex, located ~35 km to the SE of Ardnamurchan, given the geochemical similarities and previously identified laterally propagating regional dyke swarm extending to the SE of Mull.
2. Host rock lithology and pre-existing structure, as well as stress field interference, may significantly influence inclined sheet orientation. Due to these local structural controls, which deflect all sheet intrusions into a relatively consistent orientation, it is likely that only techniques sensitive to magma flow or magma source composition may differentiate centrally and laterally fed inclined sheets.
3. It is plausible that mapped abundance variations in inclined sheet swarms correspond to differing magma sources.
4. Inclined sheets cannot be projected down-dip to define a central source without first evaluating the likely position of the magma source and the structural controls on intrusion.
5. Volcanic edifice construction may be significantly influenced by magmatic processes associated with adjacent central complexes. As such, geographical proximity does not necessarily imply magmatic cogenesis. Importantly, observed evidence of edifice construction and potential eruption precursors may have resulted from, or instigate, magmatic activity in laterally adjacent volcanic systems.

Acknowledgements

Craig Magee is funded by a Natural Environment Research Council Ph.D. studentship (NER/S/A/2008/85478). Particular thanks to Ray Macdonald and an anonymous reviewer for their insightful suggestions. Thanks also to Simon Day and an anonymous reviewer for providing constructive feedback on a previous version of this

manuscript. Thanks also to Mike Petronis for helpful insights and discussions and to Ray Magee and Paul Hands for aid in sample preparation. Trevor Potts is thanked for his generous hospitality.

Appendix A. Supplementary data

Supplementary data related to this article can be found at http://dx.doi.org/10.1016/j.jsg.2012.08.004.

References

Acocella, V., Neri, M., 2009. Dyke propagation in volcanic edifices: overview and possible developments. Tectonophysics 471, 67–77.

Ancochea, E., Brandle, J.L., Huertas, M.J., Cubas, C.R., Hernan, F., 2003. The felsic dikes of La Gomera (Canary Islands): identification of cone-sheet and radial dyke swarms. Journal of Volcanology and Geothermal Research 120, 197–206.

Anderson, E.M., 1936. Dynamics of formation of cone-sheets, ring-dykes, and cauldron subsidence. Proceedings of the Royal Society of Edinburgh 56, 128–157.

Anderson, E.M., 1951. The Dynamics of Faulting and Dyke Formation with Applications to Britain. Oliver and Boyd, Edinburgh, 206 pp.

Annen, C., 2009. Implications of incremental emplacement of magma bodies for magma differentiation, thermal aureole dimensions and plutonism–volcanism relationships. Tectonophysics 500, 3–10.

Archanjo, C.J., Launeau, P., Bouchez, J.L., 1995. Magnetic fabric vs. magnetite and biotite shape fabrics of the magnetite-bearing granite pluton of Gameleiras (Northeast Brazil). Physics of the Earth and Planetary Interiors 86, 63–75.

Aubourg, C., Giordano, G., Mattei, M., Speranze, F., 2002. Magma flow in subaqueous rhyolitic dikes inferred from magnetic fabric analysis (Ponza Island, W. Italy). Physics and Chemistry of the Earth 27, 1263–1272.

Aubourg, C., Tshoso, G., Le Gall, B., Bertrand, H., Tiercelin, J.–J., Kampunzu, A.B., Modisi, M., 2008. Magma flow revealed by magnetic fabric in the Okavango giant dyke swarm, Karoo igneous province, northern Botswana. Journal of Volcanology and Geothermal Research 170, 247–261.

Baer, G., 1995. Fracture propagation and magma flow in segmented dykes: field evidence and fabric analysis, Makhtesh Ramon, Israel. In: Baer, G., Heinmann, A.A. (Eds.), Physics and Chemistry of Dykes. Balkema, Rotterdam, pp. 125–140.

Bailey, E.B., Clough, C.T., Wright, W.B., Richey, J.E., Wilson, G.V., 1924. Tertiary and Post-tertiary Geology of Mull, Loch Aline, and Oban. In: Memoir of the Geological Survey of Great Britain, Sheet 44, Scotland, 445 pp.

Bascou, J., Camps, P., Dautria, J.M., 2005. Magnetic versus crystallographic fabrics in a basaltic lava flow. Journal of Volcanology and Geothermal Research 145, 119–135.

Borradaile, G.J., Jackson, M., 2004. Anisotropy of magnetic susceptibility (AMS): magnetic petrofabrics of deformed rocks. In: Martin-Hernandez, F., Luneberg, C., Aubourg, C., Jackson, M. (Eds.), Magnetic Fabric: Methods and Applications. Geological Society of London Special Publication 238, pp. 299–360.

Bott, M.H.P., Tuson, J., 1973. Deep structure beneath the tertiary volcanic regions of Skye, Mull and Ardnamurchan, north-west Scotland. Nature Physical Science 242, 114–117.

Burchardt, S., 2008. New insights into the mechanics of sill emplacement provided by field observations of the Njardvik Sill, Northeast Iceland. Journal of Volcanology and Geothermal Research 173, 280–288.

Burchardt, S., Gudmundsson, A., 2009. The infrastructure of Geitafell volcano, Southeast Iceland. In: Thordarsson, T. (Ed.), Studies in Volcanology: The Legacy of George Walker. Geological Society of London Special Publication of IAVECI 2, pp. 349–370.

Burchardt, S., Tanner, D.C., Troll, V.R., Krumbholz, M., Gustafsson, L.E., 2011. Three-dimensional geometry of concentric intrusive sheet swarms in the Geitafell and the Dyrfjöll volcanoes, eastern Iceland. Geochemistry, Geophysics, Geosystems 12 (Q0AB09). http://dx.doi.org/10.1029/2011GC003527.

Callot, J.P., Guichet, X., 2003. Rock texture and magnetic lineation in dykes: a simple analytical model. Tectonophysics 366, 207–222.

Callot, J.P., Geoffroy, L., Aubourg, C., Pozzi, J.P., Mege, D., 2001. Magma flow direction of shallow dykes from the East Greenland margin inferred from magnetic fabric studies. Tectonophysics 335, 313–329.

Cañón-Tapia, E., 2004. Anisotropy of magnetic susceptibility of lava flows and dykes: a historical account. In: Martín-Hernández, F., Lüneburg, C.M., Aubourg, C., Jackson, M. (Eds.), Magnetic Fabric: Methods and Applications. Geological Society, London Special Publications 238, pp. 205–225.

Cañón-Tapia, E., Chávez-Álvarez, M.J., 2004. Implications for the anisotropy of magnetic susceptibility of dykes. In: Martín-Hernández, F., Lüneburg, C.M., Aubourg, C., Jackson, M. (Eds.), Magnetic Fabrics Methods and Applications. Geological Society, London, Special Publications 238, pp. 227–249.

Correa-Gomes, L.C., Souza Filho, C.R., Martins, C.J.F.N., Oliviera, E.P., 2001. Development of symmetrical and asymmetrical fabrics in sheet-like igneous bodies: the role of magma flow and wall-rock displacements in theoretical and natural cases. Journal of Structural Geology 23, 1415–1428.

Cruden, A.R., Launeau, P., 1994. Structure, magnetic fabric and emplacement of the Archean Lebel Stock, SW Abitibi Greenstone belt. Journal of Structural Geology 16, 1481–1486.

Curtis, M.L., Riley, T.R., 2003. Mobilization of fluidized sediment during sill emplacement, western Dronning Maud Land, east Antarctica. Antarctic Science 15, 393–398.

Day, S.J., 1989. The geology of the Hypersthene Gabbro of Ardnamurchan Point and its implications for its evolution as an upper crustal basic magma chamber. Ph.D Thesis. University of Durham.

Delaney, P.T., Pollard, D.D., Ziony, J.I., Mckee, E.H., 1986. Field relations between dikes and joints: emplacement processes and paleostress analysis. Journal of Geophysical Research: Solid Earth and Planets 91, 4920–4938.

Dunlop, D.J., Özdemir, O., 1997. Rock Magnetism: Fundamentals and Frontiers. Cambridge Studies in Magnetism. Cambridge University Press, New York, 573 pp.

Durrance, E.M., 1967. Photoelastic stress studies and their application to a mechanical analysis of the tertiary ring-complex of Ardnamurchan, Argyllshire. Proceedings of the Geologists' Association 78, 289–318.

Emeleus, C.H., 2009. Ardnamurchan Central Complex, Bedrock and Superficial Deposits. In: 1:25 000 Geology Series. British Geological Survey. scale 1:25 000, 1 sheet.

Emeleus, C.H., Bell, B.R., 2005. British Regional Geology: The Palaeogene Volcanic Districts of Scotland, fourth ed. British Geological Survey, Nottingham, 214 pp.

England, R.W., 1988. The early tertiary stress regime in NW Britain: evidence from the patterns of volcanic activity. In: Morgan, A.C., Parson, L.M. (Eds.), Early Tertiary Volcanism and the Opening of the NE Atlantic. Geological Society of London Special Publication 39, pp. 381–389.

Ernst, R.E., Baragar, W.R.A., 1992. Evidence from magnetic fabric for the flow pattern of magma in the MacKenzie giant radiating dyke swarm. Nature 356, 511–513.

Ernst, R.E., Head, J.W., Parfitt, E., Grosfils, E., Wilson, L., 1995. Giant radiating dyke swarms on Earth and Venus. Earth-Science Reviews 39, 1–58.

Gautneb, H., Gudmundsson, A., Oskarsson, N., 1989. Structure, petrochemistry and evolution of a sheet swarm in an Icelandic central volcano. Geological Magazine 126, 659–673.

Gautneb, H., Gudmundsson, A., 1992. Effect of local and regional stress fields on sheet emplacement in West Iceland. Journal of Volcanology and Geothermal Research 51, 339–356.

Geist, D., White, W., Naumann, T., Reynolds, R., 1999. Illegitimate magmas of the Galapagos: insights into mantle mixing and magma transport. Geology 27, 1103–1106.

Geldmacher, J., Haase, K.M., Devey, C.W., Garbe-Schönberg, C.D., 1998. The petrogenesis of tertiary cone-sheets in Ardnamurchan, NW Scotland: petrological and geochemical constraints on crustal contamination and partial melting. Contributions to Mineralogy and Petrology 131, 196–209.

Geoffroy, L., Aubourg, C., Callot, J.P., Moreira, M., 2002. Is the common use of AMS in mafic dykes scientifically correct? Terra Nova 14, 183–190.

Geshi, N., 2005. Structural development of dyke swarms controlled by the change of magma supply rate: the cone sheets and parallel dyke swarms of the Miocene Otoge igneous complex, Central Japan. Journal of Volcanology and Geothermal Research 141, 267–281.

Glazner, A.F., Bartley, J.M., Coleman, D.S., Gray, W., Taylor, R.Z., 2004. Are plutons assembled over millions of years by amalgamation from small magma chambers? GSA Today 14, 4–11.

Grandin, R., Socquet, A., Binet, R., Klinger, Y., Jacques, E., de Chabalier, J.–B., King, G.P.C., Lasserre, C., Tait, S., Tapponier, P., de Delorme, A., 2009. September 2005 Manda Hararo–Dabbahu rifting event, Afar (Ethiopia): constraints provided by geodetic data. Journal of Geophysical Research: Solid Earth and Planets 114 (B08404). http://dx.doi.org/10.1029/2008JB005843.

Grandin, R., Jacques, E., Nercessian, A., Ayele, A., Doubre, C., Socquet, A., Keir, D., Kassim, M., Lemarchand, A., King, G.P.C., 2011. Seismicity during lateral dike propagation: insights from new data in the recent Manda Hararo–Dabbahu rifting episode (Afar, Ethiopia). Geochemistry, Geophysics, Geosystems 12. http://dx.doi.org/10.1029/2010GC003434.

Gudmundsson, A., 1995. Infrastructure and mechanics of volcanic systems in Iceland. Journal of Volcanology and Geothermal Research 64, 1–22.

Gudmundsson, A., 1998. Magma chambers modelled as cavities explain the formation of rift zone central volcanoes and their eruption and intrusion statistics. Journal of Geophysical Research: Solid Earth and Planets 103, 7401–7412.

Gudmundsson, A., 2002. Emplacement and arrest of dykes in central volcanoes. Journal of Volcanology and Geothermal Research 116, 279–298.

Gudmundsson, A., 2006. How local stresses control magma-chamber ruptures, dyke injections and eruptions in composite volcanoes. Earth-Science Reviews 79, 1–31.

Gudmundsson, A., Phillip, S.L., 2006. How local stress fields prevent volcanic eruptions. Journal of Volcanology and Geothermal Research 158, 257–268.

Herrero-Bervera, E., Walker, G.P.L., Cañón-Tapia, E., Garcia, M.O., 2001. Magnetic fabric and inferred flow direction of dykes, conesheets and sill swarms, Isle of Skye, Scotland. Journal of Volcanology and Geothermal Research 106, 195–210.

Horsman, E., Tikoff, B., Morgan, S.S., 2005. Emplacement-related fabric in a sill and multiple sheets in the Maiden Creek sill, Henry Mountains, Utah. Journal of Structural Geology 27, 1426–1444.

Hrouda, F., 2003. Indices for numerical characterization of the alteration processes of magnetic minerals taking place during investigation of temperature variation of magnetic susceptibility. Studia Geophysica et Geodaetica 47, 847–861.

Hutton, D.H.W., 2009. Insights into magmatism in volcanic margins: bridge structures and a new mechanism of basic sill emplacement – Theron Mountains, Antarctica. Petroleum Geoscience 15, 269–278.
Jackson, M.D., Pollard, D.D., 1988. The laccolith-stock controversy: new results from the southern Henry Mountains, Utah. Geological Society of America Bulletin 100, 117–139.
Jelínek, V., 1978. Statistical processing of anisotropy of magnetic susceptibility measured on groups of specimens. Studia Geophysica et Geodaetica 22, 50–62.
Jolly, R.J.H., Sanderson, D.J., 1995. Variation in the form and distribution of dykes in the Mull swarm, Scotland. Journal of Structural Geology 17, 1543–1557.
Jolly, R.J.H., Sanderson, D.J., 1997. A Mohr circle construction for the opening of a pre-existing fracture. Journal of Structural Geology 19, 887–892.
Kavanagh, J.L., Menand, T., Sparks, R.S.J., 2006. An experimental investigation of sill formation and propagation in layered elastic media. Earth and Planetary Science Letters 245, 799–813.
Kerr, A.C., Kent, R.W., Thompson, B.A., Seedhouse, J.K., Donaldson, C.H., 1999. Geochemical evolution of the tertiary Mull volcano, NW Scotland. Journal of Petrology 40, 873–908.
Keunen, P.H., 1937. Intrusion of cone sheets. Geological Magazine 74, 177–183.
Khan, M.A., 1962. The anisotropy of magnetic susceptibility of some igneous and metamorphic rocks. Journal of Geophysical Research 67, 2867–2875.
Klausen, M.B., 2004. Geometry and mode of emplacement of the Thverartindur cone sheet swarm, SE Iceland. Journal of Volcanology and Geothermal Research 138, 185–204.
Klausen, M.B., 2006. Geometry and mode of emplacement of dyke swarms around the Birnudalstindur igneous centre, SE Iceland. Journal of Volcanology and Geothermal Research 151, 340–356.
Knight, M.D., Walker, G.P.L., 1988. Magma flow directions in dikes of the Koolan Complex, Oahu, determined from magnetic fabric studies. Journal of Geophysical Research: Solid Earth and Planets 93, 4308–4319.
Kokelaar, B.P., 1992. Fluidization of wet sediments during the emplacement and cooling of various igneous bodies. Journal of the Geological Society of London 139, 21–33.
Launeau, P., Cruden, A.R., 1998. Magmatic fabric acquisition mechanisms in a syenite: results of a combined anisotropy of magnetic susceptibility and image analysis study. Journal of Geophysical Research: Solid Earth and Planets 103, 5067–5089.
Liss, D., Hutton, D.H.W., Owens, W.H., 2002. Ropy flow structures – a neglected indicator of magma flow direction in sills and dykes. Geology 30, 715–718.
Liss, D., Owens, W.H., Hutton, D.H.W., 2004. New palaeomagnetic results from the Whin Sill complex: evidence for a multiple intrusion event and revised virtual geomagnetic poles for the late Carboniferous for the British Isles. Journal of the Geological Society of London 161, 927–938.
Macdonald, R., Wilson, L., Thorpe, R.S., Martin, A., 1988. Emplacement of the Cleveland Dyke: evidence from geochemistry, mineralogy, and physical modelling. Journal of Petrology 29, 559–583.
Macdonald, R., Baginski, B., Upton, B.G.J., Dzierzanowski, P., Marshall-Roberts, W., 2009. The Palaeogene Eskdalemuir dyke, Scotland: long-distance lateral transport of rhyolitic magma in a mixed-magma intrusion. Mineralogical Magazine 73, 285–300.
Marinoni, L.B., Gudmundsson, A., 2000. Dykes, faults and palaeostresses in the Teno and Anaga massifs of Tenerife (Canary Islands). Journal of Volcanology and Geothermal Research 103, 83–103.
Mathieu, L., van Wyk de Vries, B., 2009. Edifice and substrata deformation induced by intrusive complexes and gravitational loading in the Mull volcano (Scotland). Bulletin of Volcanology 71, 1133–1148.
Mathieu, L., van Wyk de Vries, B., Holohan, E.P., Troll, V.R., 2008. Dykes, cups, saucers and sills: analogue experiments on magma intrusion into brittle rocks. Earth and Planetary Science Letters 271, 1–13.
McKeagney, C.J., Boulter, C.A., Jolly, R.J.H., Foster, R.P., 2004. 3-D Mohr circle analysis of vein opening, Indarama lode-gold deposit, Zimbabwe: implications for exploration. Journal of Structural Geology 26, 1275–1291.
Menand, T., 2008. The mechanics and dynamics of sills in layered elastic rocks and their implications for the growth of laccoliths and other igneous complexes. Earth and Planetary Science Letters 267, 93–99.
Morgan, S., Stanik, A., Horsman, E., Tikoff, B., de Saint-Blanquat, M., Habert, G., 2008. Emplacement of multiple magma sheets and wall rock deformation: Trachyte Mesa intrusion, Henry Mountains, Utah. Journal of Structural Geology 30, 491–512.
Odé, H., 1957. Mechanical analysis of the dyke pattern of the Spanish Peaks area, Colorado. Bulletin of the Geological Society of America 68, 567–576.
O'Driscoll, B., Troll, V.R., Reavy, R.J., Turner, P., 2006. The Great Eucrite intrusion of Ardnamurchan, Scotland: reevaluating the ring-dyke concept. Geology 34, 189–192.
O'Driscoll, B., Stevenson, C.T.E., Troll, V.R., 2008. Mineral lamination development in layered gabbros of the British Palaeogene Igneous Province: a combined anisotropy of magnetic susceptibility, quantitative textural and mineral chemistry study. Journal of Petrology 49, 1187–1221.
Orlický, O., 1990. Detection of magnetic carriers in rocks: results of susceptibility changes in powdered rock samples induced by temperature. Physics of the Earth and Planetary Interiors 63, 66–70.
Owens, W.H., 1974. Mathematical model studies on factors affecting the magnetic anisotropy of deformed rocks. Tectonophysics 24, 115–131.
Owens, W.H., 2000. Error estimates in the measurement of anisotropic magnetic susceptibility. Geophysical Journal International 142, 516–526.
Özdemir, O., O'Reilly, W., 1981. High temperature hysteresis and other magnetic properties of synthetic monodomain titanomagnetites. Physics of the Earth and Planetary Interiors 25, 406–418.
Özdemir, O., O'Reilly, W., 1982. Magnetic hysteresis properties of synthetic monodomain titanomaghemites. Earth and Planetary Science Letters 57, 467–478.
Palmer, H.C., Ernst, R.E., Buchan, K.L., 2007. Magnetic fabric studies of the Nipissing sill province and Senneterre dykes, Canadian Shield, and implications for emplacement. Canadian Journal of Earth Sciences 44, 507–528.
Paquet, F., Dauteuil, O., Hallot, E., Moreau, F., 2007. Tectonics and magma dynamics coupling in a dyke swarm of Iceland. Journal of Structural Geology 29, 1477–1493.
Pasquarè, F.A., Tibaldi, A., 2007. Structure of a sheet-laccolith system revealing the interplay between tectonic and magma stresses at Stardalur Volcano, Iceland. Journal of Volcanology and Geothermal Research 161, 131–150.
Petrovský, E., Kapička, A., 2007. On determination of the Curie point from thermomagnetic curves. Journal of Geophysical Research: Solid Earth and Planets 111 (B12S27). http://dx.doi.org/10.1029/2006JB004507.
Phillips, W.J., 1974. The dynamic emplacement of cone sheets. Tectonophysics 24, 69–84.
Philpotts, A.R., Philpotts, D.E., 2007. Upward and downward flow in a camptonite dike as recorded by deformed vesicles and the anisotropy of magnetic susceptibility (AMS). Journal of Volcanology and Geothermal Research 161, 81–94.
Pinel, V., Jaupart, C., 2004. Magma storage and horizontal dyke injection beneath a volcanic edifice. Earth and Planetary Science Letters 221, 245–262.
Pitcher, W.S., 1979. The nature, ascent and emplacement of granitic magmas. Journal of the Geological Society of London 71, 259–305.
Pollard, D.D., 1987. Elementary fracture mechanics applied to the structural interpretations of dykes. In: Halls, H.C., Fahrig, W.F. (Eds.), Mafic Dyke Swarms. Geological Society of Canada Special Paper 34, pp. 5–24.
Pollard, D.D., Johnson, A.M., 1973. Mechanics of growth of some laccolithic intrusions in the Henry Mountains, Utah. II. Bending and failure of overburden layers and sill formation. Tectonophysics 18, 311–354.
Richey, J.E., Thomas, H.H., 1930. The Geology of Ardnamurchan, North-west Mull and Coll. In: Memoir of the Geological Survey of Great Britain, Sheet 51 and 52, Scotland, 393 pp.
Rickwood, P.C., 1990. The anatomy of a dyke and the determination of propagation and magma flow directions. In: Parker, A.J., Rickwood, P.C., Turner, D.H. (Eds.), Mafic Dykes and Emplacement Mechanisms, pp. 81–100.
Rhodes, J.M., Wenz, K.P., Neal, C.A., Sparks, J.W., Lockwood, J.P., 1989. Geochemical evidence for invasion of Kilauea's plumbing system by Mauna Loa magma. Nature 337, 257–260.
Rubin, A.M., 1995. Propagation of magma-filled cracks. Annual Review of Earth and Planetary Sciences 23, 287–336.
Schirnick, C., van den Bogaard, P., Schmincke, H., 1999. Cone sheet formation and intrusive growth of an oceanic island – the Miocene Tejeda complex on Gran Canaria (Canary Islands). Geology 27, 207–210.
Schofield, N., Stevenson, C., Reston, T., 2010. Magma fingers and host rock fluidization in the emplacement of sill. Geology 38, 63–66.
Schofield, N., Brown, D., Magee, C., Stevenson, C.T.E., 2012. Sill morphology and comparison of brittle and non-brittle emplacement mechanisms. Journal of the Geological Society of London 169, 127–141.
Siler, D.L., Karson, J.A., 2009. Three-dimensional structure of inclined sheet swarms: implications for crustal thickening and subsidence in the volcanic rift zones of Iceland. Journal of Volcanology and Geothermal Research 188, 333–346.
Speight, J.M., Skelhorn, R.R., Sloan, T., Knaap, R.J., 1982. The dyke swarms of Scotland. In: Sutherland, D. (Ed.), Igneous Rocks of the British Isles. Wiley, Chichester, New York, pp. 449–459.
Stevenson, C.T.E., Owens, W.H., Hutton, D.H.W., Hood, D.N., Meighan, I.G., 2007a. Laccolithic, as opposed to cauldron subsidence, emplacement of the Eastern Mournes pluton, N. Ireland: evidence from anisotropy of magnetic susceptibility. Journal of the Geological Society of London 164, 99–110.
Stevenson, C.T.E., Owens, W.H., Hutton, D.H.W., 2007b. Flow lobes in granite: the determination of magma flow direction in the Trawenagh Bay Granite, northwestern Ireland, using anisotropy of magnetic susceptibility. Bulletin of the Geological Society of America 119, 1368–1386.
Tarling, D.H., Hrouda, F., 1993. The Magnetic Anisotropy of Rocks. Chapman and Hall, New York, 217 pp.
Tauxe, L., 1998. Paleomagnetic Principles and Practice. In: Modern Approaches in Geophysics, vol. 17. Kluwer Academic Publishers, Dordrecht, Boston, London.
Tauxe, L., Gee, J.S., Staudgiel, H., 1998. Flow directions in dikes from anisotropy of magnetic susceptibility data: the bootstrap way. Journal of Geophysical Research: Solid Earth and Planets 103, 17775–17790.
Thomson, K., 2007. Determining magma flow in sills, dykes and laccoliths and their implications for sill emplacement mechanisms. Bulletin of Volcanology 70, 183–201.
Tibaldi, A., Pasquarè, F.A., 2008. A new mode of inner volcano growth: the "flower intrusive structure". Earth and Planetary Science Letters 271, 202–208.
Tibaldi, A., Pasquarè, F.A., Rust, D., 2011. New insights into the cone sheet structure of the Cuillin complex, Isle of Skye, Scotland. Journal of the Geological Society of London 168, 689–704.
Walker, G.P.L., 1975. A new concept of the evolution of the British Tertiary intrusive centres. Journal of the Geological Society of London 131, 121–141.

Walker, G.P.L., 1993. Re-evaluation of inclined intrusive sheets and dykes in the Cuillins volcano, Isle of Skye. In: Prichard, H.M., Alabaster, T., Harris, N.B.W., Neary, C.R. (Eds.), Magmatic Processes and Plate Tectonics. Geological Society of London Special Publication 76, pp. 489–497.

Wall, M., Cartwright, J., Davies, R., McGrandle, A., 2009. 3D imaging of a tertiary dyke swarm in the Southern North Sea, UK. Basin Research 22, 181–194. http://dx.doi.org/10.1111/j.1365-2117.2009.00416.x.

White, R.S., 1992. Magmatism during and after continental break-up. In: Storey, B.C., Alabaster, T., Pankhurst, R.J. (Eds.), Magmatism and Causes of Continental Break-up. Geological Society, London, Special Publications 68, pp. 1–16.

Zellmer, G.F., Annen, C., 2008. An introduction to magma dynamics. In: Annen, C., Zellmer, G.F. (Eds.), Dynamics of Crustal Magma Transfer, Storage and Differentiation. Geological Society, London, Special Publication 304, pp. 1–13.